

5-1-2024

Investigative Research on Design Parameters and Criticality Models for Microreactors

Cameron Jensen

Follow this and additional works at: <https://digitalscholarship.unlv.edu/thesesdissertations>



Part of the [Mechanical Engineering Commons](#), and the [Nuclear Engineering Commons](#)

Repository Citation

Jensen, Cameron, "Investigative Research on Design Parameters and Criticality Models for Microreactors" (2024). *UNLV Theses, Dissertations, Professional Papers, and Capstones*. 5014.
<http://dx.doi.org/10.34917/37650837>

This Thesis is protected by copyright and/or related rights. It has been brought to you by Digital Scholarship@UNLV with permission from the rights-holder(s). You are free to use this Thesis in any way that is permitted by the copyright and related rights legislation that applies to your use. For other uses you need to obtain permission from the rights-holder(s) directly, unless additional rights are indicated by a Creative Commons license in the record and/or on the work itself.

This Thesis has been accepted for inclusion in UNLV Theses, Dissertations, Professional Papers, and Capstones by an authorized administrator of Digital Scholarship@UNLV. For more information, please contact digitalscholarship@unlv.edu.

INVESTIGATIVE RESEARCH ON DESIGN PARAMETERS AND CRITICALITY MODELS
FOR MICROREACTORS

By

Cameron Jensen

Bachelor of Science in Engineering – Mechanical Engineering
University of Nevada, Las Vegas
2022

A thesis submitted in partial fulfillment
of the requirements for the

Master of Science – Materials and Nuclear Engineering

Department of Mechanical Engineering
Howard R. Hughes College of Engineering
The Graduate College

University of Nevada, Las Vegas
May 2024



Thesis Approval

The Graduate College
The University of Nevada, Las Vegas

February 2, 2024

This thesis prepared by

Cameron Jensen

entitled

Investigative Research on Design Parameters and Criticality Models for Microreactors

is approved in partial fulfillment of the requirements for the degree of

Master of Science – Materials and Nuclear Engineering
Department of Mechanical Engineering

Alexander Barzilov, Ph.D.
Examination Committee Co-Chair

Charlotta Sanders, Ph.D.
Examination Committee Co-Chair

Jeremy Cho, Ph.D.
Examination Committee Member

Richard Gardner, Ph.D.
Graduate College Faculty Representative

Alyssa Crittenden, Ph.D.
*Vice Provost for Graduate Education &
Dean of the Graduate College*

Abstract

With increased energy demand and the desire to reduce reliance on fossil fuels, nuclear power will need to play a prominent role in achieving carbon-free energy independence. Large nuclear reactors are necessary to meet this objective. However, they are expensive and take a long time to build. For remote locations (e.g., military bases) and smaller communities, large nuclear reactors would not be feasible or cost effective. Small reactors (microreactors) can fill this necessary gap. These reactors would be factory-built, delivered quickly, and operated with high intrinsic levels of safety. With microreactors still in conceptual and testing states, there is a large need to study how these reactors produce consistent energy in a much smaller package.

The objective of this research is to develop design parameters and criticality models for a reactor core that can be used in a microreactor, which would self-regulate based on automatic control functions. This research investigates parameters and constraints for the reactor design, including a reactor core fueled with TRISO fuel, different cooling methods, and graphite moderators. Sensitivity studies are conducted on temperature, fuel depletion, and criticality control methods, and an enrichment of 20% U-235 will be used as the primary source of heat. A core achieving a critical state with temperatures ranging from room temperature to 1200K is considered. Feedback mechanisms are also investigated, including inherently safe fuel design and control rod manipulation.

Acknowledgements

First, I would like to thank my advisor, Dr. Charlotta Sanders, who has continuously guided and supported me throughout my entire graduate program. I am grateful for the flexibility and patience she has granted me while working in unique and often challenging remote conditions.

Next, I am thankful for my committee members, Dr. Alexander Barzilov, Dr. Jeremy Cho, and Dr. Richard Garner for their unique contributions not only through my thesis work but through my graduate degree. These professors have made my experience the best it can be and have given me a learning environment I not only felt comfortable in, but will look back on with fond memories.

I would also like to thank my family for the constant support and reminders that anything is possible when I set my mind to it. They have given me the opportunity to pursue an advanced degree and have encouraged me the entire way.

Lastly, I would like to acknowledge and dedicate this thesis to my fiancé, Lana Kojoian. If everyone had someone this supportive, encouraging, kind, and caring in their life, the world would be a much better place. In the hardest of moments, Lana has only ever lifted me up and left me wondering why I questioned my abilities in the first place. I will forever be grateful to have met my best friend in what has been the most academically challenging time of my life.

Table of Contents

Abstract	iii
Acknowledgements	iv
Table of Contents	v
List of Tables:	viii
List of Figures:	ix
Chapter 1. Introduction	1
1.1. Background Information	1
1.2. The Future of Nuclear Power	3
1.3. Current Projects	4
1.4. Selection of Modeled Components	8
1.5. Objectives of the Thesis	9
1.6. The Structure of this Thesis	10
Chapter 2. Methodology	11
2.1. Monte Carlo Calculations	11
2.1.1. Six-Factor Formula	12
2.1.2. Temperature Effects on Reactivity	14
2.1.2. Monte Carlo N-Particle (MCNP) Code Description	16
2.1.3. Benchmark Evaluations	16
2.2. Reactor Design	19
2.2.1. Assumptions Made	21
2.2.2. Homogenization Process	25
2.2.3. Defense in Depth	27

2.3 Input MCNP File Design	28
2.31. Cell Card	28
2.32. Surface Card	31
2.33. Burn Card	31
2.34. Material/Data Card	32
2.35. Tally Card	34
2.4. Data Collection Process	34
2.5. Core Layout	34
Chapter 3. Data Collection and Analysis Given MCNP Data	38
3.1. Desired Outcome	38
3.2. Range of Inputs Tested	38
3.21. Temperature Variation	38
3.22. Pitch Variation	39
3.23. Moderator Variation	39
3.24. Size Variation	40
3.25. Power Variation	40
3.26. Control Rod Variation	40
3.3. Calculational Data	41
3.31 Variations in Reactor Component Temperatures	41
3.32 Burnup Calculation Analysis	46
3.4. Data Analysis	53
Chapter 4. Conclusion	56
4.1. Conclusion	56

4.2. Suggested Future Work	57
Appendix A: Density Homogenization Calculations	58
Appendix B: Upper Safety Limit Development	59
Appendix C: Input Files	63
Appendix D: Output Results Matrix	77
Appendix E: Tally Case Results	85
Bibliography	95
Curriculum Vitae	100
Specialized Skills/Strengths	100
Education	100
Engineering Experience	100

List of Tables:

Table 1.1: Very Small Reactor Designs Being Developed up to 25 Mwe	6
Table 1.2: Initial Microreactor Design Study	7
Table 2.1: Top Ten Benchmark Cases for Air Cooled Moderator Input File	18
Table 2.2: Assumptions Made for Investigative Criteria	22
Table 2.3: Thickness and Density for TRISO Particle Layers	26
Table 3.1: Variations in Air Temperature for Criticality Analysis	42
Table 3.2: Variations in Sodium Temperature for Criticality Analysis	43
Table 3.3: Variations in Water Temperature for Criticality Analysis	43
Table 3.4: Variations in Graphite Temperature for Criticality Analysis	44
Table 3.5: Variations in Fuel Temperature for Criticality Analysis	45
Table 3.6: Spectrum Percentage for Neutron Fission	53
Table A.1: Material Density Calculations	58
Table A.2: Material Card Percentages	58
Table D.1: Size Comparisons	77
Table D.2: Control Rod Comparison	77
Table D.3: Comparison of Fuel Levels	77
Table D.4: Control Rod Enrichment Comparison	78

List of Figures:

Figure 1.1: Nuclear Reactor Power Comparisons by the Department of Energy	2
Figure 2.1: Estimation of Monte Carlo Errors	12
Figure 2.2: Resonance Broadening due to the Doppler Effect	15
Figure 2.3: Fuel Components from Fuel Kernel to Fuel Block	20
Figure 2.4: Layers of a TRISO Pebble	26
Figure 2.5: Microreactor Core Layout in XY Plane	35
Figure 2.6: Microreactor Core Center in XY Plane	35
Figure 2.7: Microreactor Core Layout in XZ Plane	36
Figure 3.1: Burnup Results at 5 MW With No Control Rod Insertion	47
Figure 3.2: Burnup Results at 5 MW With Control Rod Insertion	49
Figure 3.3: Burnup Summary of Most Reactive Case (Mat=1200 K, Fuel= 900k)	51
Figure 3.4: Neutron Reaction Probabilities in Natural Uranium and Graphite	54
Figure D.1: Burnup Results at 2.5 MW With No Control Rod Insertion	79
Figure D.2: Burnup Results at 5 MW With No Control Rod Insertion	80
Figure D.3: Burnup Results at 7 MW With No Control Rod Insertion	81
Figure D.4: Burnup Results at 2.5 MW With Control Rod Insertion	82
Figure D.5: Burnup Results at 5 MW With Control Rod Insertion	83
Figure D.6: Burnup Results at 7 MW With Control Rod Insertion	84

Chapter 1. Introduction

As the next generation of nuclear power plants are quickly becoming more of a reality, the need for research into these reactors is critical. As demand grows for smaller, more remote sources of power, microreactors are looking to demonstrate that nuclear power can infiltrate markets previously untouched. With these reactors being rapidly developed, more studies are needed to prove the fuel source can consistently and efficiently provide energy and remain critical given smaller physical footprints. As there is no existing database for built microreactors and their specifications (primarily because none have been constructed yet), this thesis will help fill that gap and provide building blocks for what constitutes successful reactor core design. To achieve this, criticality studies with core design elements are analyzed using industry standard software and proven analysis methods to compare a range of different materials and conditions a reactor may face while in use. These dose calculations, material analysis, and heat transfer analysis establish a baseline for future expectant work in this area. In conclusion, this work will explain the means to control criticality given a small core, analyze current design trends with several methods of moderation and reactivity feedback mechanisms, and provides expected performance results over the span of a core's lifetime.

1.1. Background Information

From the discovery of nuclear fission, scientists worldwide have steadily built on developed historical knowledge to provide humankind with one of the most efficient, cleanest, and safest sources of power. Communities who will benefit the most from new nuclear technologies, such as microreactors, are developing countries due to limited financial sources, countries with limited land or natural resources that may not be able to expansively use

sustainable power sources such as solar and wind, and the remote or mobile military applications. With 92 nuclear reactors in 28 states, around 19% of America's electricity is currently produced via nuclear fission (DOE, 2021). Over 27 countries currently operate nuclear plants and 17 have plans to introduce nuclear power into their grids (Gralla, 2017).

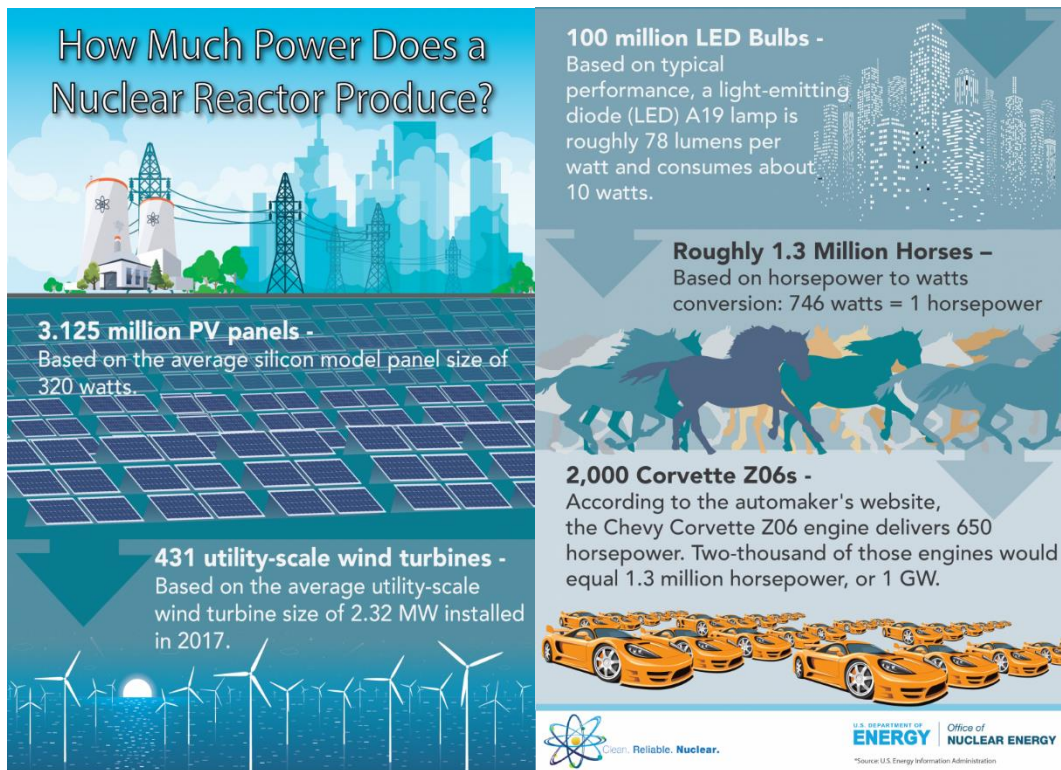


Figure 1.1: Nuclear Reactor Power Comparisons by the Department of Energy

For rural small communities, microreactors could be fundamental towards reducing energy access inequality, as rural towns often struggle with producing their own electricity and must have it delivered via the power grid connected to external states, making them financially reliant on the larger communities and corporations nearby (Macdonald, 2019). One megawatt of

energy (1000KW) is roughly enough energy to meet the demand of 750 homes at once in current day America (California ISO, 2023) and self-produced energy via a microreactor could offer a solution to this issue, allowing towns to be self-reliant for their energy needs.

Additionally, military applications in remote and unestablished places often need large amounts of energy to create temporary bases and power equipment, frequently at short notice (GAO, 2009). Nuclear microreactors offer a great solution to these problems, providing a much more deployable source. These small reactors are defined as supplying 1-20 MWe, operating as part of the electric grid or completely independent from it (Beneš, 2021). The fundamental design and technological application for microreactors is similar to previous generation reactors: they feature a nuclear fuel core of some form of Uranium-235 that undergoes fission to create heat which in turn powers a steam turbine. This fundamental process has remained the same since the earliest of reactor designs (such as the EBR-1 Reactor) and does not necessarily need to be proven again in microreactor designs (INL, 2023), and is therefore not considered within this thesis work. Although the energy production process is similar, design priorities have also evolved to include the focus to make these plants self-sustaining while simultaneously incorporating enhanced safety features to prevent an accident without the aid of an operator (Sugawara, 2023). However, no criticality analysis has been completed on an operating microreactor design due to a lack of operational reactors.

1.2. The Future of Nuclear Power

America's long history with building large reactors has shown significant costs overruns due to the required build time, and their complexity. Recently, the Georgia Power Vogtle 3 reactor began producing energy after years of construction delays due to supply chain challenges,

design changes, and license amendments (Robb, 2023). The nuclear industry will not be a viable energy generating source should this trend of building delays and cost overruns limit the number of energy markets nuclear is able to serve. In this way, microreactors may be a solution to these fiscal challenges. Microreactors would also allow the nuclear industry to compete evenly with other energy generating sources, while also maintaining certain advantages over diesel generators and renewable sources in microgrids including reductions in CO₂ production, “always on” energy production, and much smaller production facility footprints (Testoni, 2021).

Microreactors can be a leading example in changing the nuclear mindset by creating factory reproducible modules that will drastically decrease time from proposal to finished product. To achieve the goals set forth by microreactor designers, the core must serve as the center of an intrinsically safe, reliable source of heat. This thesis looks to identify what this core will look like in microreactors and give insight as to what components designers should account for when designing their own core.

1.3. Current Projects

Many microreactor designs are currently in the conceptual design stage. The Advanced Reactor Demonstration Program (ARDP), a 2020 competition sponsored by the Department of Energy, is supporting ten different advanced reactor designs, three of which have already received over a billion dollars in funding (GAO, 2022). These projects include the X-Energy Xe-100 Demonstration (\$1.2B USD), the NuScale Carbon Free Power Project (\$1.35B USD), and the Terra Power Sodium Demonstration (\$1.97B USD). These companies have prioritized the creation of small modular reactors (SMR’s) to help solve the energy and climate crisis in

America. These funds are being distributed towards both new SMR technology designs, as well as advanced microreactor designs.

Another large government backed contribution is Project PELE, a Department of Defense funded program created in 2016 (Walkman, 2022). This program focuses on the research of new energy developments for use by the United States Military to meet the need for a new mobile power source. This microreactor focused program has chosen and funded BWX Technologies to work with the Idaho National Laboratory (INL) and build the first microreactor in the United States in 2024 (Walkman, 2022). BWXT has partnered with Northrop Grumman, Aerojet Rocketdyne, and others to get the reactor built and fueled and will undergo up to three years of testing at INL. The project is expected to be valued around \$300 million. In September of 2023, Project PELE was also expanded to include the XE-Mobile, X-Energy's microreactor as well (X-Energy, 2023). In the United States alone, several billion dollars have been invested in the development of new microreactor technology.

While much information remains proprietary for designs, most microreactor design companies have at least released a basic fact sheet of their units' outputs, fueling methods, cooling methods, and current development stages. The World Nuclear Association has composed a list of the current designs in development as seen in Table 1.1.

Table 1.1: Very Small Reactor Designs Being Developed up to 25 Mwe (WNA,2023)

Name	Capacity	Type	Developer
U-battery	4 MWe	HTR	Urenco-led consortium, UK
Starcore	10-20 MWe	HTR	Starcore, Quebec
MMR-5/-10	5 or 10 MWe	HTR	UltraSafe Nuclear, USA
Holos Quad	3-13 MWe	HTR	HolosGen, USA
Gen4 module	25 MWe	Lead-bismuth FNR	Gen4 (Hyperion), USA
Xe-Mobile	1-5 MWe	HTR	X-energy, USA
BANR	50 MWt	HTR	BWXT, USA
Sealer	3-10 MWe	Lead FNR	LeadCold, Sweden
eVinci	0.2-5 MWe	Heatpipe FNR	Westinghouse, USA
Aurora	1.5 MWe	Heatpipe FNR	Oklo, USA
NuScale micro	1-10 MWe	Heatpipe	NuScale, USA

The most developed designs have been summarized in Table 1.2. These designs will help define starting conditions and boundaries of what a microreactor core should consist of.

Table 1.2: Initial Microreactor Design Study

Reactor	Country of Origin	MWe Capacity	Fuel Type	Cooling Method	Ease of Setup/Disposal	Current Development Stage
E-Vinci (Westinghouse,2024)	USA	5 MW	TRISO	Passive heat pipe, Sodium	30 days on site install. Reactor removed for refueling.	Design Stages, commercial deployment aimed for 2027.
Starcore (Starcore Nuclear,2022)	CA	20 MW	TRISO	High Temp Gas (Helium)	Portable, no setup times available	License to construct by 2027.
Project Pele BWXT (Waksman,2020)	USA	5 MW	TRISO	Passive heat pipe	72-hour setup,7-day teardown	Delivering for testing to INL in 2025. Have started TRISO fuel production.
Sealer -Leadcold (Wallenius,2017)	SWE	10 MW	Low Enriched UO2	Lead FNR	To be determined	In licensing stages.
Xe-Mobile (X-Energy,2024)	USA	7 MW	TRISO	High Temp Gas	Truck ready, within days set up. Construction in 3-6 Months	In prototype stages, will develop further with Project Pele funding.
MMR (Ultra Safe Nuclear, 2023)	USA	10 MW	TRISO	High Temp Gas	Assembly in months, decommission in 1 year	Demonstration Units planned for 2026.

There are several common trends among the new reactors, including TRISO based fuel, high-temperature gas cooling, and operational status within the second half of the decade. Current microreactor designs have been influenced from existing research conducted on High Temperature Gas Reactors (HTGR), which were historically successful beginning with the Peach Bottom Reactor 1 built in the 1960’s as well as the modern designs HTTR and HTR-10 (McDowell, 2015). These include using high operating temperatures in prismatic shapes with gas

cooled cores. Among the initial microreactor design study, the Project Pele BWXT reactor stands out as the most design ready. Unfortunately, this also comes with most design information remaining proprietary as it is the leader in development and will be used for United States Armed Forces applications. This includes any kind of criticality studies done by neutronics teams.

With a focus on criticality control, Monte Carlo simulations in MCNP-6 will be used to create models with several different components inspired by Table 1.1. Section 1.4 explores the different core characteristics, which systems are influenced by existing designs, and what boundaries should be used when analyzing the results.

1.4. Selection of Modeled Components

While microreactors can have several systems to support operation, modeling the entire reactor, for the needs of this study, would be too complex and computationally time consuming expensive for the purpose of establishing the wanted design parameters. Also, creating too specific of an input would limit the study when asking to establish a baseline configuration for different design concepts. Using common design features between concepts is key to establishing a usable database. For this thesis, everything within the designed concrete shell boundary has been included in Monte Carlo calculations, including the fuel source, a moderator, a reflector, and a cooling method. These are the different components considered relevant when looking within the Monte Carlo analysis.

Criticality of the core is met when the number of neutrons created due to fission is equal to the number of neutrons being absorbed. This balance creates the consistent, controlled energy that is demanded from power plants. If the number of neutrons produced is less than that being absorbed, the reactor is left in a state of subcriticality in which no chain reaction occurs. If more

neutrons are produced than absorbed, fission occurs but at an uncontrolled, increasing rate (NRC, 2011). This is unwanted because the reaction is no longer controlled and can result in serious harm to both human life and the environment (Cardis, 2011). In many criticality accidents, human error is the leading cause (McLaughlin, 2000). As an example, the Three Mile Island accident in 1979 has been extensively studied, and Bot et al. (2003) claims that the reactor would have safely shut down if not for the operator actions. To help resolve these human errors, generation IV reactors are focused on creating passive systems, focusing on the fuel source and cooling. Fuels are being designed to prevent meltdowns and have a built-in containment system within the protective layers (X-energy 2024). Passive cooling systems such as reactor cavity cooling systems and passive heat transfer pipes require little to no support systems to remove dependencies on support systems (Ultra Safe, 2023). This thesis accounts for these fuel and heat pipes and models these for criticality studies.

1.5. Objectives of the Thesis

The objective of this research is to develop design parameters and criticality models for a reactor core that can be used in a microreactor, which would self-regulate based on automatic control functions. This research investigates parameters and constraints for the reactor design, including a reactor core fueled with TRISO fuel, different cooling methods, and graphite moderators. Sensitivity studies are conducted on temperature, fuel depletion, and criticality control methods. An enrichment of 20% U-235 is used as the primary source of heat. A core achieving a critical state with temperatures ranging from room temperature to 1200K is considered. Feedback mechanisms are also investigated, including inherently safe fuel design and control rod manipulation.

Using these constraints, an initial design is suggested for use in the beginning stages of microreactor conceptual design. Furthermore, this thesis looks to narrow down what factors play the largest roles in criticality design when investigating microreactors specifically and what changes must be made to design when working at a smaller level of energy production.

1.6. The Structure of this Thesis

Chapter 2 discusses the experimental methodology. It entails the type of code used for criticality calculations, the assumptions made for calculation purposes, the development of an upper safety limit, the experimental design inputs, data collection process, uncertainty analysis, and criticality information.

Chapter 3 discusses the data acquired through Monte Carlo calculations and visualization information on several different kinds of core manipulations. A mixture of different variables are evaluated to create a core database.

Chapter 4 is the conclusion. It includes the suggestions that are drawn from calculations and analysis as well as future suggested work. The appendices include supplemental data from the study.

Chapter 2. Methodology

2.1. Monte Carlo Calculations

Monte Carlo calculations are one of the most widely used tools to assess criticality both during design and operation stages for nuclear power plants (Haghighat, 2021). These calculations are based on probabilistic, repetitive, random sampling to obtain a result. This is especially helpful when tracking the path of a neutron, which is the particle of interest that can travel in any direction of the XYZ plane from its source. Depending on where the neutron travels, its interactions can include absorption and reflection off the materials around it. Monte Carlo uses a random number generator to determine path length, interaction type, and scattering angle if applicable (Haghighat, 2021). Repeating this process millions of times eventually builds a model given all events for a neutron produced from its source. By doing this, an accurate result can be reached to predict how the core will behave. When done by hand, these calculations can be tedious and have large errors. Even though these are predictions, several steps are taken in Monte Carlo calculations and software to create more precise results, reducing the uncertainty. Figure 2.1 highlights the principle of increasing the number of runs in Monte Carlo simulations. In a well-behaved tally, the relative error is proportional to one over the square root of the number of histories. To halve relative error, the total number of histories must be increased fourfold.

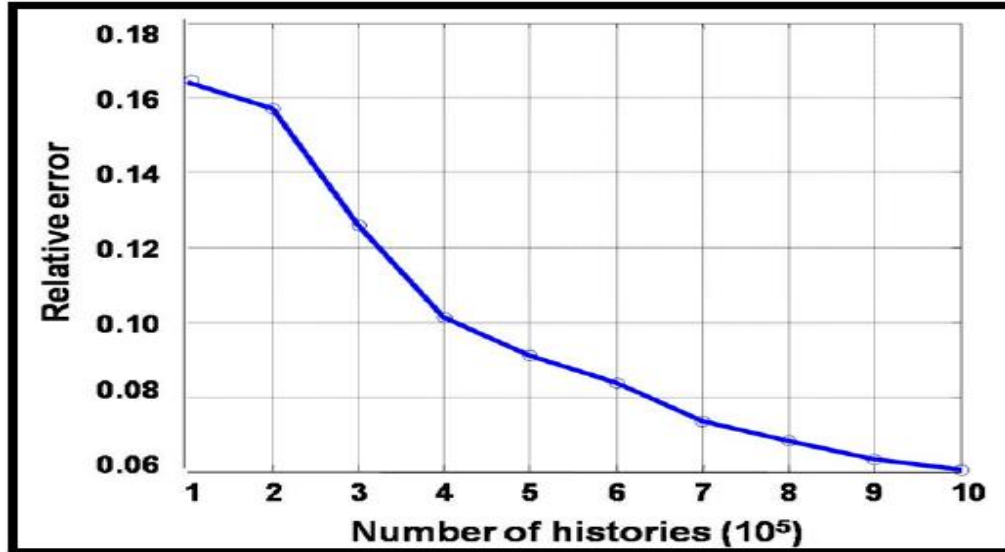


Figure 2.1: Estimation of Monte Carlo Errors

2.11. Six-Factor Formula

With a goal of producing constant power, the rate at which neutrons are produced and absorbed by the system must be in equilibrium. When neutrons are born, the majority are born in the fast region. From here, the neutrons can either leak out of the reactor, have fast fission, or continue to slow down. As the neutrons slow down, they pass through resonance regions (where they can be captured) and then become thermal. They can then leak out of the reactor as thermal leakage or be captured and fission. The ratio of how frequently these events occur defines criticality. The average effective multiplication factor, k_{eff} , is the multiplication factor ratio of current neutron population to the previous population (Koreshi, 2022). Values below 1 are deemed subcritical, in which the production of neutrons is outweighed by the number of neutrons absorbed. Values above 1 are undesirable as more neutrons are produced than absorbed, creating

a potentially unstoppable chain reaction. A value of 1 is the primary objective inside nuclear reactors to meet equilibrium and consistently create power (Koreshi, 2022). This relationship is modeled in reactor physics as the six-factor formula, shown below.

$$k_{eff} = k_{\infty} P_T P_f$$

The effective multiplication factor is equal to the infinite media multiplication factor multiplied by the thermal non leakage and fast non leakage probabilities. These leakage probability terms are relevant when given a specific sized reactor with defined geometry barriers and must be considered when calculating the effective multiplication factor. k_{∞} is representative of criticality given infinite size, considering no leakage. Considering this thesis uses a thick concrete reflector, the probability that no leakage occurs is very close to 1. This allows the leakage terms to be removed and k_{eff} set equal to k_{∞} . This term can be further broken down into the four-factor formula shown below, which is used for infinite size cases (Koreshi, 2022).

$$k_{\infty} = \frac{\rho \epsilon \eta_T f \Sigma_a \phi_T}{\Sigma_a \phi_T} = \eta_T f \rho \epsilon$$

As each component is altered, there will be a shift in system criticality. Each of these factors are described as the following:

η_T is the reproduction factor. This factor is the ratio of fast neutrons produced by thermal fission to the number of thermal neutrons absorbed in the fuel. This factor is especially important for uranium as it increases with enrichment.

f is the thermal utilization factor, or the fraction of absorbed neutrons in the fuel. This describes how effectively thermal neutrons are absorbed in the fuel, rather than absorption to other core materials.

ρ is the resonance escape probability factor. This is the fraction of neutrons that escape resonance capture, slowing from the fast energy range to the thermal energy range. This factor is especially susceptible to change from doppler broadening, in which broader resonances will increase capture percentages.

ϵ is the macroscopic cross section factor, or the fast fission factor. It is the ratio of fast neutrons produced by fissions at all energies to the number of fast neutrons produced in thermal fission. (Lamarsh, 2001). As materials in this thesis are investigated, the four-factor equation will provide insight on the fundamental understanding of why reactivity changes and how each condition contributes to this equation.

2.12. Temperature Effects on Reactivity

As part of this thesis, temperature variation was essential in properly analyzing performance. As reactors undergo variation in temperature during operation, materials must uphold their physical properties to prevent meltdown and cause a gap in containment. Materials also must be analyzed to observe how temperature impacts intrinsic properties that could influence reactivity. This is especially important for the fuel and moderator materials, as temperature can drastically change neutron cross sections. This is especially true considering the negative temperature coefficient of reactivity. This coefficient relates temperature to reactivity within a specific material, where a negative coefficient means as temperature rises, reactivity decreases (Lamarsh, 2001). This is an inherent safety feature of reactors. When coolant is removed and the temperature of a core increases, the fuel will become less reactive.

This negative temperature coefficient is due to the nuclear Doppler effect. Neutron cross sections experience resonances at certain energies, where at colder temperatures, these

resonances are sharp spikes and inefficient at absorbing neutrons. As temperature begins to increase, these same resonances become wider and shorter, becoming more absorbent as neutrons slow down through the energy spectrum towards the thermal range (Lamarsh, 2001). This decreases criticality as more neutrons are absorbed into the material. While individual materials might have a negative temperature coefficient, the overall temperature coefficient depends on design layout and combined material factors and might not replicate that of the fuel source. Figure 2.2 shows an example of this spread of a resonance given different temperature.

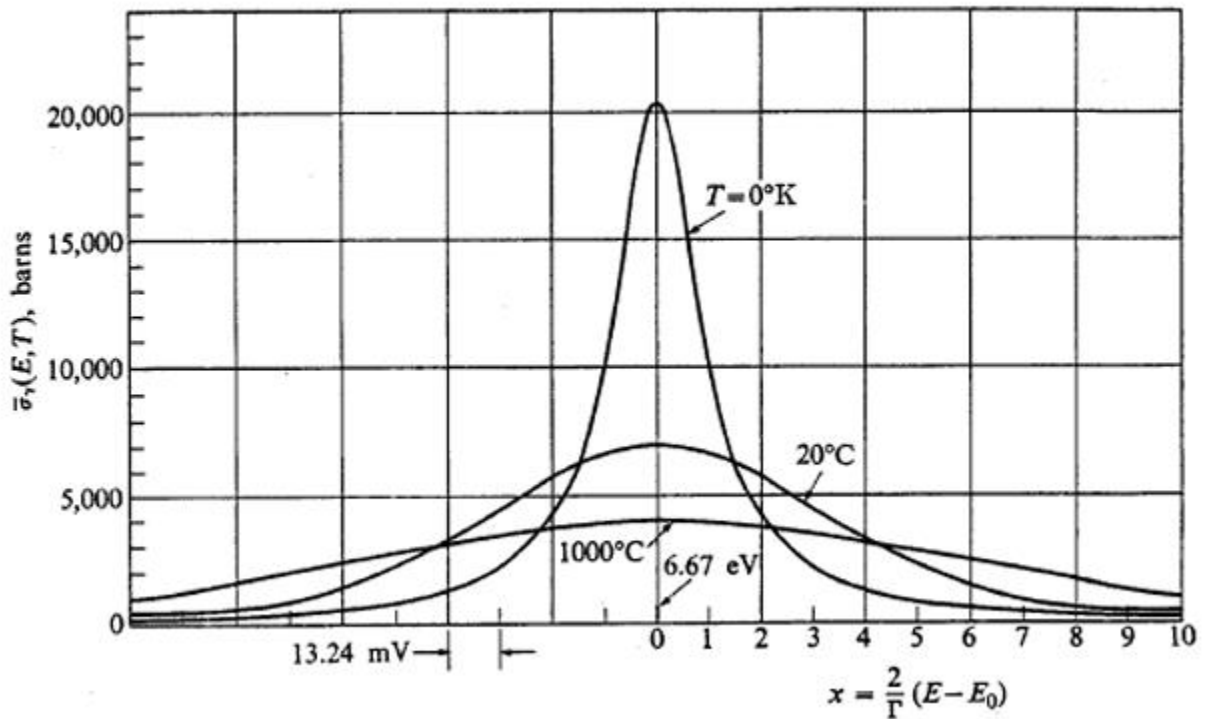


Figure 2.2: Resonance Broadening due to the Doppler Effect (Greenwood, 1997)

2.12. Monte Carlo N-Particle (MCNP) Code Description

Monte Carlo N-Particle-6, or MCNP6, was used as the validation method for all the calculations used in this thesis. The program was installed from the CD-ROM supplied by the Radiation Safety Information Computational Center (RSICC) onto a home desktop. The code is updated to the most current 2023 edition. All calculations were executed under the `xmdir_mcnp6.2` directory, which invokes the modules for cross section preparation. Version ENDF/B-VII.1 cross sections were used exclusively in this NSCE as the default data. Verifying the code's correct installation was completed by running the set of sample problems provided with the MCNP package and the International Handbook of Evaluated Criticality Safety Benchmark Experiments and confirming agreement with the reference output files.

The MCNP6 code has been validated through comparison to known critical experiments (NEA, 2020). In addition to previous studies, the program has been validated using volume V of *The International Handbook of Evaluated Criticality Safety Benchmark Experiments*. These include shapes, compositions, and testing conditions within an area of applicability for the fissile mixture being evaluated. To be considered a valid case of comparison, several areas of applicability need to be assessed, as found in Tables 2.3 and 2.5 of NUREG-6698 (NRC,2001).

2.13. Benchmark Evaluations

To further establish confidence within the MCNP code, a benchmark study was completed using existing baseline experiments in the MCNP6 application. This was done via Whisper, a statistical analysis package included in the MCNP6.2 download (Brown, 2017). Whisper uses the sensitivity profile data generated via MCNP 6 and automatically compares the data to existing nuclear cross-section covariance data and catalog of sensitivity profiles for more

than 1100 experiments. Upon completion, a correlation coefficient is generated, used to compare benchmarks to the new microreactor core design. Although Whisper provides “repeatable, quantitative, physics-based information to NCS analysts for determining upper safety limits”, special consideration must be given to correlation coefficients developed in the output files of whisper (Brown, 2017). The correlation coefficient is a ratio of shared uncertainty between two models. This value, defined as C_k , measure similarity between an input file and existing benchmark data. This is done on a scale of 0 to 1.0, with 1.0 being an identical match (Maldonado, 2023). As a rule of thumb, only existing designs with a value of 0.90 correlation coefficient should be considered neutronically similar and valid for the development of uncertainty analysis. Whisper cases were completed for several input files varying in coolant method and temperature. Table 2.1 shows the benchmark cases considered for development with its associated correlation coefficient. The top ten cases are shown for air cooled cases, with the rest of the data available in Appendix B. Between all three cooling methods, there was no noticeable change in C_k values with all values being below 0.81.

Table 2.1: Top Ten Benchmark Cases for Air Cooled Moderator Input File

Benchmark Case	Ck value
heu-sol-therm-042-006.i	0.8067
heu-sol-therm-042-004.i	0.8059
heu-sol-therm-042-005.i	0.8056
heu-sol-therm-042-007.i	.08047
heu-sol-therm-032-001.i	0.8022
heu-sol-therm-042-003.i	0.8019
heu-sol-therm-042-008.i	0.8001
heu-sol-therm-020-004.i	0.7792
heu-sol-therm-042-002.i	0.7791
heu-sol-therm-021-004.i	0.7739

A review of the Whisper runs shows that no Ck value is higher than 0.8067, which is not close enough to the 0.90 desired similarity rating. It is determined that there is not enough comparable benchmark information to change the k_{eff} critical value. Whisper 1.1, the most updated version, only includes data from 2016 and does not yet feature similar microreactor core designs (Brown, 2017). For this reason, an assumption is made that output k_{eff} generated for this thesis must be studied for values close to 1.0.

2.2. Reactor Design

Tri-structural Isotropic particle fuel (TRISO) is highly regarded as the “most robust nuclear fuel on earth” by the Department of Energy (2023), with TRISO particles unable to melt in a commercial high-temperature reactor during recent testing at Idaho National Laboratory. The fuel can achieve three times the burnup current light-water fuels can achieve, much to the benefit of remote microreactors which will need to run years without refueling (Marciulescu, 2019). The fuel is featured in several new microreactor designs, including Ultra Safe Nuclear’s Micro Modular reactor, X-Energy’s XE-Mobile reactor, and the Project Pele BWXT reactor. For the proposed model being studied in this thesis, Uranium-235 fuel will be examined with a value of 20% enrichment in the form of uranium dioxide (UO₂). TRISO fuel is complex in its design, including several protective layers only micrometers wide. A single kernel consists of fuel composed of uranium dioxide approximately eight hundred micrometers in diameter. This kernel is surrounded by several layers, including a buffer layer of air to allow for expansion, a pyrolytic carbon (PyC) layer 35um thick, a silicon carbide layer 36um thick, and an outer PyC layer 20um thick. Each of these layers plays a vital role in protecting nuclear material and serves as an excellent passive safety system. The fuel can safely reach temperatures of 1800 degrees Kelvin and still maintain its form (UNSC, 2023). While different production facilities may have slightly different thicknesses of these layers, the general layout of the kernel remains the same.

In prismatic designs, thousands of these poppy seed sized pebbles are inserted into a silicon carbide matrix, creating a fully ceramic micro-encapsulated fuel (FCM). This combination creates “an extremely rugged and stable fuel with extraordinarily high temperature stability” (UNSC, 2023). Figure 2.3 visualizes the packing formation of these TRISO pebbles in the UNSC reactor.

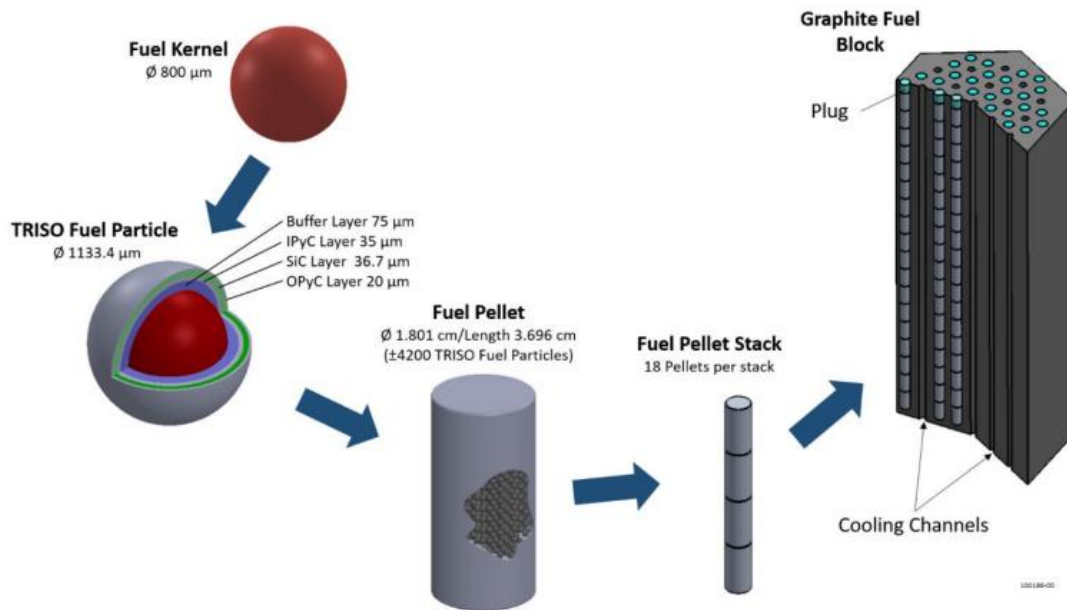


Figure 2.3: Fuel Components from Fuel Kernel to Fuel Block (USNC, 2023)

In pebble bed reactors, these kernels are packed into billiard ball sized pebbles and thousands are laid loosely together inside of the reactor core. Packing fraction is crucial to criticality as it determines how much fuel is located inside the core related to other neutron absorbing materials. In pebble beds, early tests have shown that a 62-63% packing fraction is achievable, specifically in further developed SMR designs (Brown, 2022). This packing fraction, however, can change given seismic events, as pebbles might shift and change the packing fraction and thus criticality. For prismatic reactors, packing fractions are also estimated to be around the same, 60%, with seismic events not being as much of a concern due to the fuel pellets being held in place. In this thesis, a prismatic design has been chosen to be modeled in MCNP for criticality testing. The packing fraction of this fuel is assumed to be 60% for the purpose of

consistency across the tests. The FCM cylinder-shaped fuel pellets are small, often around 4cm in diameter and 8cm in length. Exact measurements depend on the fuel manufacturer and often remain proprietary. These pellets are then stacked to form fuel rods and inserted into a fuel block, complete with a graphite moderator/reflector structure and cooling channels. The fuel block often follows a similar grid pattern across designs, considering spacing requirements and accessibility for maintenance and refueling, if desired (UNSC,2023). Around the outer edge, concrete surrounds the structure as the final reflector of the core.

2.21. Assumptions Made

To design a TRISO-based microreactor core, several key components must be considered. These include the fuel source, the moderator, the methods of cooling, the type of structure holding the fuel, and the surrounding container. While a range of different technologies might be present inside the reactor, this thesis only examines the criticality of the core itself, assuming other infrastructure is outside the scope of this thesis and will impact criticality on a case-by-case basis. With TRISO fuel and microreactors still in the initial stages of commercial use, some assumptions are made due to the classified technology, as well as limited data from live tests. Table 2.2 provides a summary of assumptions made, with a more detailed description below.

Table 2.2: Assumptions Made for Investigative Criteria

	Assumption	Engineering Judgement/Justification
Assumption 1	Homogenized TRISO pellet layers	Brown (2005) confirmed the usage of homogenization for TRISO fuel acceptable for Monte Carlo calculations, given certain conditions.
Assumption 2	Height of the core is four meters	Standard height of four meters chosen given conceptual designs and requirement to fit in shipping container.
Assumption 3	Core temperature is evaluated between room temperature and 1200 Kelvin.	Based on available cross section information for selected materials, MCNP defined data can be used for material cards.
Assumption 4	Material selection	Materials are all sourced from <i>Compendium of Material Composition Data for Radiation Transport Modeling</i> (Detwiler,2021)
Assumption 5	Power Level	Output levels are to be evaluated at 3 possible levels given existing microreactor designs.
Assumption 6	Only criticality factors from defined materials	Assume negligible effect from other materials outside of the established core space due to focus on core design.
Assumption 7	A k_{eff} value of 1 is considered critical.	Due to insufficient Whisper correlation coefficient results, a k_{eff} of 1.0 is considered the point of criticality.
Assumption 8	Test conditions with a wide delta in graphite/fuel temperatures with the rest of the reactor will not be considered for burnup studies.	While certain cases might have extreme differences in temperature (near 900k difference) these cases are not likely for long term usage as various heat transfer will keep temperatures within the reactor to temperatures closer to equilibrium.

Assumption 1: Homogenized TRISO Pellet Layers.

Fuel pellets provide complex geometry and require a large amount of computing power when doing criticality studies (Brown, 2022). A core fully modeled with tens of thousands of TRISO particles would be unnecessary given the negligible benefits. Homogenization of the fuel source has been considered as a solution. Brown concludes that homogenization can introduce a

large error (over 5%) to criticality results when the entire TRISO particle is homogenized but if just the UO₂ is left unhomogenized, there is a significant decrease in computing time with no significant effect on the results (± 0.004 difference in k_{eff} when compared to a heterogeneous core with the same cubic lattice structure). This thesis utilizes the homogenization process within the input file, smearing fuel coatings together to separate the fuel and the graphite matrix from the coatings. While small amounts of accuracy in criticality calculations might be sacrificed, it is negligible when compared to the computational time gained back. This serves as a much more efficient method to conduct tests and collect data for several different core configurations. The homogenization process for input is explained in Section 2.22.

Assumption 2: Core Height is Four Meters.

While a specific height is not required for criticality, a consistent height is chosen to focus on lattice manipulation when investigating geometry. This height is assumed to be 4 m, a value consistent with concepts (Beneš, 2021). This height provides a good benchmark for tests and will fit into a shipping container for easy transportation.

Assumption 3: Core Temperature.

To match available cross section data from the MCNP Manual Appendix G, the temperature of the core was investigated in several conditions, ranging from room temperature up to 1200 K, still below the limit of the TRISO particle fuel (Trejo, 2022). Testing done at room temperature, 600k, 900k, and 1200k gives a good variation in possible reactor temperatures.

Assumption 4: Material Selection.

The qualities of non-fuel related materials have been pulled from the *Compendium of Material Composition Data for Radiation Transport Modeling* (Detwiler, 2021). This U.S. Department of Homeland Security sponsored document serves as an established location to grab

material information including chemical compositions, material mixture ratios and densities for criticality studies. Using this document as a source creates consistent, trackable material data supported by those directly involved with the development of MNCP 6. For TRISO fuel in specific, the Ultra Safe Nuclear TRISO/FCM Fuel pellets were used as a guideline. As one of the most market-ready, tested, and commercial types of TRISO fuel available, this source provided an accurate description of all layers relevant to the core design.

Assumption 5: Power Level.

It can be assumed that for criticality burnup calculations, the reactor will be running at full power year-round. While there is no data available yet for online time for microreactors, it will be assumed that they will work perfectly, capturing the highest amount of burnup over time. This best-case scenario will be conservative in measuring burnup given the reactor does have downtime during operation.

Assumption 6: Criticality Factors from Defined Materials.

Besides the materials included in this report, it is to be assumed that there will be a negligible effect on criticality from outside materials. If other materials were to be included, the complexity of the system would increase computational run times and remove the generalizations this reactor core assumes. This research helps to investigate a starting point that a specialized criticality design can continue to build upon.

Assumption 7: k_{eff} of 1.0 Considered Critical.

Based on the benchmark evaluations made in section 2.12, not enough benchmark cases showed enough neutronic similarity to build an upper safety limit. More benchmark data is needed to develop a proper upper safety limit and thus a value of 1.0 will remain as the best

safety limit available. Cases around this value, both above and below 1.0, will be considered when studying critical cases. This will account for some uncertainty in calculations.

Assumption 8: Temperature Gap.

Certain results studied can produce critical values while having extreme differences in temperatures. An example of this is a fuel temperature of 293.6K, but a graphite temperature of 1200k. With energy being removed from the reactor primarily from conduction and convection, surrounding materials will constantly be out of thermal equilibrium at this large temperature difference (Lamarsh, 2001). For long term analysis, this is not realistic as the entropy of the system will increase over time and temperatures will not remain at these consistent temperatures. Engineering judgement is used to establish what temperatures are considered extreme.

2.22. Homogenization Process

Instead of modeling each individual TRISO particle, the core can be homogenized by theoretically separating the uranium fuel and combining the similar coating layers together. Using this theory, the materials are less geometrically complicated and smearing the fuel coatings into the graphite matrix has no significant effect on results, running about 30% faster than the cases that explicitly model the fuel coatings (Brown, 2005).

To homogenize the layers, calculations had to be made using existing TRISO particle data from manufacturers and plant designers. While this information is often classified, several online sources including USNC and Project Pele give general TRISO particle size approximations. Depending on the manufacturer and design criteria, there could be a range in which produced particles are sized, giving some variances in standard TRISO design criteria. Due to its availability and maturity of design, the existing 500-micrometer kernel design from USNC was

chosen to represent the parameters of the TRISO fuel. These values are shown in Table 2.3 with a diagram of a particle shown in Figure 2.3.

Table 2.3: Thickness and Density for TRISO Particle Layers

Layers	Thickness(um)	density(g/cc)
UO ₂ Kernel diameter	800	10.8
Buffer	75	0.98
Inner PyC coating	35	1.85
SiC layer coating	36.7	3.2
Outer PyC coating	20	1.86

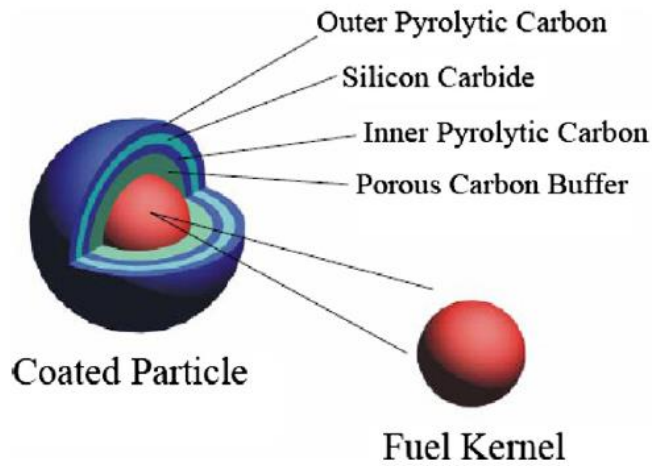


Figure 2.4: Layers of a TRISO Pebble (USNC)

Using the thicknesses of each layer, the percentage of the total particle volume of each material can be solved for. This is useful in creating the ratio of fuel to buffer layers. The packing fraction of particles into FCM pellets must also be accounted for. This also gives data for how much of each buffer layer is included in material two, the combined buffer layer material. Once layers combine, an average density of the material can be determined (Brown, 2005). Appendix A highlights the calculations used for Materials 1 and 2 data.

2.23. Defense in Depth

While achieving criticality is the goal for energy production, there is a need to also control reaction and ensure the safety of the users and the environment. Several layers of defense are designed into the reactor. The first layer of defense is the negative temperature reactivity coefficients seen within the fuel. As temperature rises in the core, the fuel experiences a change in cross sections. This change impacts the ability of the fuel to absorb the neutrons, which leads to a decrease in reactivity. This also helps lower reactivity in case of a heat spike, especially because other materials inside the reactor have temperature reactivity coefficients different than the fuel that could increase reactivity (Lamarsh, 2001). Because the core is homogenized, true temperature coefficients might act differently as fuel layers play an important role in preventing meltdowns.

The second layer of defense is the control rods. These rods are controlled by a control rod drive mechanism that automatically maintains the critical levels of the reactor given normal transients. The mechanism is also set up to automatically drop control rods into the system in case of emergency conditions. This case is later analyzed with MCNP in Chapter 3.

The third layer of defense is the fuel core geometry itself. Previous generations of fuel were at risk of melting surrounding reactor materials at very high temperatures and causing meltdowns. TRISO fuel features several protective layers designed to withstand temperatures well above 1200K, preventing fuel from escaping its pebbles and combining to meltdown (Trejo, 2015). These safety features combine to encourage many companies to deem their microreactors ‘walk away safe’ (Baumer, 2010). These layers of defense are considered in the input files via Section 2.34 Material/Data card as well as 3.26 Control Rod Variation.

2.3 Input MCNP File Design

All MCNP 6 input files share a similar structure with several key components needed to define geometry, materials, and testing conditions. The breakdown of each “card” of the material is listed below.

2.31. Cell Card

The cell card begins on the first line after the title in an MCNP input file and uses inputs from the surface card and material card to establish how the core is constructed. Each line consists of a different component type within the core and has the following layout:

```
8 0 -10.96 -4 5 -6 u=1 tmp=2.529E-08 IMP:N=0 IMP:P=1 $ inner cask void
```

The 8 defines the cell number, with cells listed on the card in numerical order, beginning with surface 1. The 0 represents the material that the cell is filled with; in this case, 0 represents a void. The -10.96 represents the density of the cell, with a positive value indicating atomic density in units of 10^{24} atoms/cm³ and a negative value indicating mass density in g/cm³ units.

When testing at different temperatures, proper material density must be accounted for. Materials such as water will experience large changes in density across temperature compared to that of graphite. The -4,-5, and -6 define where Cell 8 geometry is located within the model. Depending on the definitions in the surface card, these numbers can represent different shapes or planes. From this example, Cell 8 is inside of Shape 4, above Plane 5 and below Plane 6. u represents the universe the cell is in, which establishes a reusable configuration of geometry, materials, and densities of combined cells. Tmp represents the thermal temperature of the cell, converted to units of MeV. When testing at different temperatures, this element is essential to ensure individual cells are tested at the correct temperature. IMP represents the importance of the cell related to neutrons (N) and protons (P). Depending on the transport problem, one or both might be set to a Boolean importance of 1. For this thesis, only neutron tracking is necessary for criticality purposes. The dollar sign indicates that a comment has begun on the line, with any characters appearing after used purely for description; they will not give any input for calculation. MCNP6.2 allows only 128 characters per line, so descriptions must be continued on the next line with a c character to begin to prevent errors. Extra comments within the card can be started on any line of the card if they have the c character at the beginning of the line.

In many MCNP models, there can be several hundred repetitive geometries, given the repetitive nature of core components. To quickly describe a core, universes can be established and repeated given a lattice. The lattice cell from this microreactor thesis is shown below.

10 7 -2.25 -7 8 -9 10 u=4 imp:n=1 lat=1 fill=-9:9 -9:9 0:0 \$square lattice-cell

```

4 4 4 4 4 4 4 4 4 4 4 4 4 4 4 4 4 4 4 4
4 4 4 4 4 4 4 4 4 4 4 4 4 4 4 4 4 4 4 4
4 4 4 4 4 4 4 4 4 4 4 4 4 4 4 4 4 4 4 4
4 4 4 1 1 1 1 1 1 1 1 1 1 1 1 1 1 4 4 4
4 4 4 1 1 1 1 1 1 1 1 1 1 1 1 1 1 4 4 4
4 4 4 1 1 2 1 1 1 1 1 1 1 2 1 1 4 4 4
4 4 4 1 1 1 1 1 1 1 1 1 1 1 1 1 4 4 4
4 4 4 1 1 1 1 2 1 1 1 2 1 1 1 1 4 4 4
4 4 4 1 1 1 1 1 1 1 1 1 1 1 1 1 4 4 4
4 4 4 1 1 1 1 1 1 3 1 1 1 1 1 1 4 4 4
4 4 4 1 1 1 1 1 1 1 1 1 1 1 1 1 4 4 4
4 4 4 1 1 1 1 2 1 1 1 2 1 1 1 1 4 4 4
4 4 4 1 1 1 1 1 1 1 1 1 1 1 1 1 4 4 4
4 4 4 1 1 1 1 1 1 1 1 1 1 1 1 1 4 4 4
4 4 4 1 1 2 1 1 1 1 1 1 2 1 1 4 4 4
4 4 4 1 1 1 1 1 1 1 1 1 1 1 1 1 4 4 4
4 4 4 1 1 1 1 1 1 1 1 1 1 1 1 1 4 4 4
4 4 4 4 4 4 4 4 4 4 4 4 4 4 4 4 4 4 4 4
4 4 4 4 4 4 4 4 4 4 4 4 4 4 4 4 4 4 4 4
4 4 4 4 4 4 4 4 4 4 4 4 4 4 4 4 4 4 4 4

```

The cell begins the same, with the cell number (10), cell material number (7), and the density of the material (-2.25). This material fills the entire space defined within Universe 4. Added to this card is the lattice (lat=1) and is sized using the fill card. The dimensions of the fill are defined via a range in the X, Y, and Z planes. In the following lines, the lattice is filled using the existing universes defined in the cell cards. This can take up many rows in the file, but each universe entered can represent several complex geometries and drastically save design time. Although the cell card is first chronologically, it is often best to begin by building the surfaces and the surface materials so building blocks are available when creating cells.

2.32. Surface Card

The surface card defines all the needed physical geometry to create boundaries and build the reactor in MCNP6. MCNP offers a Surface Card dictionary within the manual, featuring the card entry structure for numerous shapes including planes, spheres, cylinders, and surfaces defined by points. All the input files studied include cylinders centered around the Z axis as well as planes in the X, Y, and Z directions. A sample surface is listed below, shown as surface 1 cylinder centered on the Z axis with its point locations on the x and y axis and radius in centimeters.

```
1 C/Z 5 5 10 $ a cylindrical surface parallel to z-axis
```

2.33. Burn Card

To analyze the performance of a reactor over time at a given power level, a burn card must be included in the input file. The burn card used for this thesis is listed below.

```
BURN TIME= 365 365 365 365 MAT = 1 Power =5.0  
BOPT=1.0 11 1 OMIT=1,8,6014,7016,8018,9018,13026,13028,14027,16031
```

The BURN signals the beginning of information related to the burnup calculations. Burnup is measured by running a criticality calculation at different time steps and analyzing the different elements produced due to reactions within the reactor, such as Xenon. Due to these reactions in the fuel, credit can be taken for the reduction in reactivity, often called burnup credit (Sanders, 2001). The production of these elements decreases criticality overtime and helps guide reactor operators as to when fuel needs to be changed. TIME represents the amount of time that passes between burnup measurements and criticality calculations, in this case 365-day periods for

a total of four years. One measurement is also taken at the beginning of the year for fresh fuel information. The MAT card calls out which fissile material from the material card is to be analyzed for burnup. The volume must be included in the cells that the material is into accurately account for the mass of fissile material present. Power represents the level at which the reactor is running in megawatts. BOPT sets the optional conditions for the test, including the amount of fission products included, what to include in the output file, and how to interpret cross-section data. Based on the cross-section data included, the OMIT card might need to be used to remove certain isotopes from fission products due to cross section not being available in the MCNP repositories. For this input file, 8 isotopes were excluded to complete calculations, all deemed acceptable as there is no transport cross section data available. (Los Alamos, 2009)

2.34. Material/Data Card

The material/data card defines the composition of all components within the input file. An example of Material 1 from this thesis is listed below.

```
m1  92235.83c 0.202 $Uranium 235 inside fuel kernel rho=10.96 g/cm^3, enrichment 6%,  
T=293.6k  
  
8016.83c 2.0 $Oxygen inside fuel kernel+PyC  
92238.83c 0.798 $Uranium 238 inside fuel kernel  
  
mt1  o2-u.20t
```

Materials begin with an m before the number of the material used. In case the material contains a treatment such as oxygen within the uranium, MT must be added in front of the 1 (Werner, 2017)). This can be required when materials have different cross section behavior, such as how oxygen can behave differently when mixed with uranium rather than by itself in the

thermal regime (MCNP 2018). The element number follows with the atomic number, followed by up to three digits for the atomic mass number, which is especially useful when calling for specific isotopes of an elements. After these digits, a period separates the cross-section specification. This cross-section specification is crucial to correct calculations, especially given the behavior of cross sections when running cases at different temperatures. There are several material libraries to reference that are downloaded automatically with MCNP. Appendix G is used to ensure that all materials are collected from the same source. This thesis utilizes the ENDF71x library from ENDF/B-VII.1 (LANL, 2011). To establish the composition of a material with several elements, the fraction is listed after the library, either as an atomic fraction (positive) or weight fraction (negative).

At the end of the card is the information given to generate output tables and set the conditions for testing. The criticality code is given below.

```
kcode 7500 1 150 550 $ KCODE (# of Neutrons/Cycle) (Initial keff guess) (# of skipped cycles)(# of total cycles)
```

While there are many data cards available for printing, criticality studies begin with KCODE, or the criticality source. This will print several relevant tables when examining a criticality study. The testing conditions follow, which establish the number of neutrons run per cycle, the initial k_{eff} guess, the number of skipped cycles, and the number of total cycles. These four variables help establish enough runs to ensure that results follow a normal distribution, confidence levels are at acceptable levels, enough neutrons are captured, and criticality numbers are precise. This data card was used across different input files as test results were deemed acceptable.

2.35. Tally Card

The tally card instructs MCNP what specific data to provide given the Monte Carlo Calculation. Current across a surface, flux at a specific point, cross section data, and many other factors can be provided by these cards. To examine cross section data, the standard tallies (F) card was used as well as the tally multiplier to generate information across volumes. An example of a tally card is given as F4:N 1 The F4 card provides the flux averaged over a cell in units of neutrons/cm². Material one is selected as the tested cell. A tally multiplier card FM can also be added to multiply any tallied quantity by cross section to give many relevant reaction rates, such as elastic and total fission cross section.

2.4. Data Collection Process

To gather useful data, hundreds of MCNP input files have been created and run to create a plethora of information. MCNP generates output files that can be converted to .TXT for data collection. Before data is collected, verification of a successful run is checked via warning comments (or lack thereof), normal distribution at confidence levels, and component information. Final k_{eff} values are extrapolated from these files as well as burnup information from files that include the burn card. Data is then stored in an excel spreadsheet for easier manipulation.

2.5. Core Layout

Given the experimental setup information from Chapter 2, a base core was developed in MCNP. Figures 2.5, 2.6, and 2.7 below show the core in the XY plane and the XZ plane as seen from the MCNP Visual Editor (Schwarz, 2018).

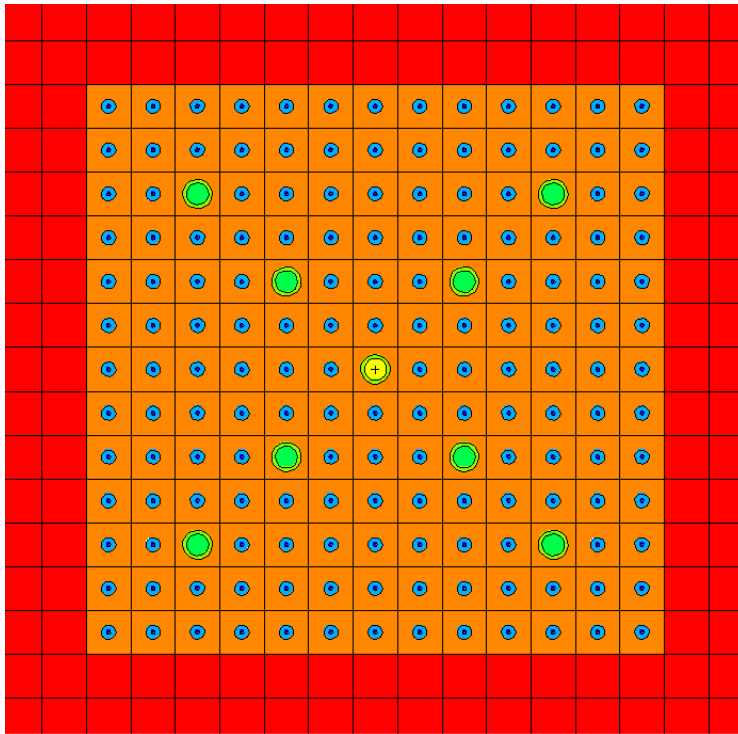


Figure 2.5: Microreactor Core Layout in XY Plane

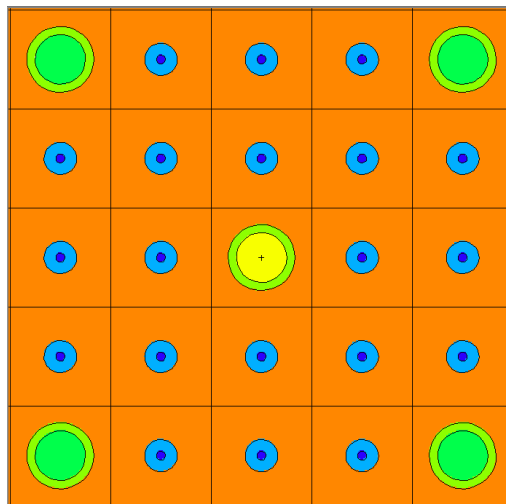


Figure 2.6: Microreactor Core Center in XY Plane

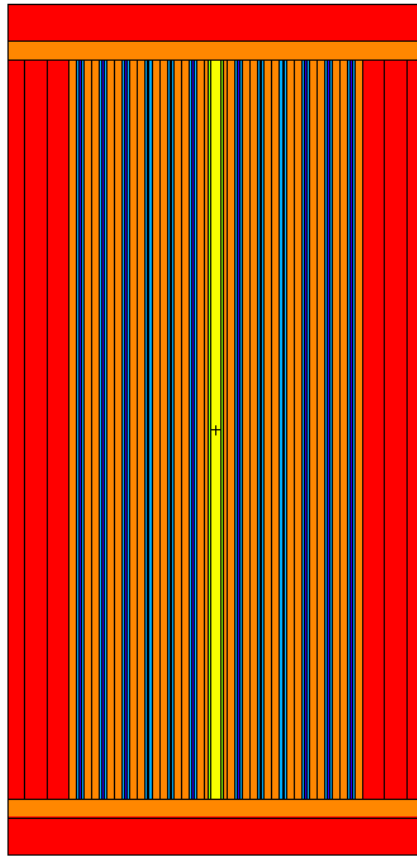


Figure 2.7: Microreactor Core Layout in XZ Plane

The following colors represent the following materials:

Red: The concrete shell around the outside of the reactor. While there are materials outside of this barrier, primarily for radiation shielding to protect the operator, an assumption has been made that concrete can be the boundary of the core. A full microreactor design would need to incorporate other systems to properly distribute energy and operate properly.

Orange: The graphite moderator and structural component holding all relevant piping in place. This graphite makes up much of the material in the core.

Light Green: Makes up the steel pipes containing different moderators as well as the zirconium hydride.

Green: The moderator flow area, either air, sodium, or water. This also serves as the place control rods are inserted into.

Yellow: The zirconium hydride center. This serves as a central, added moderator with the added hydrogens flowing down fast neutrons.

Light Blue: The combined layers of the TRISO buffers. The size of these reflects the volume ratios of buffers to fuel.

Purple: Isolated UO₂ Fuel at 20% enrichment. There are 160 of these rods in total.

Chapter 3. Data Collection and Analysis Given MCNP Data

3.1. Desired Outcome

In determining what is considered a successful design, several key factors must be considered. A successful reactor design should meet all objectives established for this thesis, in addition to the following guidelines:

- Materials must not melt at extreme temperatures and survive until the fuel requires changing.
- k_{eff} values should remain at critical levels as established by uncertainty analysis until the desired microreactor lifespan is reached
- Reactor must respond to control rods and reach a subcritical state to meet supercriticality defense measures.

3.2. Range of Inputs Tested

Once a ‘base’ design was set for the microreactor, the manipulation of inputs began. Using existing microreactor designs, variations were added to temperature, materials, size, and output power, with all being measured against criticality. Each of these variations was studied individually and is explained in the following sections.

3.2.1. Temperature Variation

Different temperatures were evaluated across all inputs as the reactor must survive in a range of different conditions, from a cold start up to a loss of coolant accident. Temperatures

were selected given available cross section data from appendix g for all materials in the material cards (Werner, 2017). Temperatures and their associated cross sections from the ENDF71x library were used including 293.6K (.80c), 600.0K(.81c), 900.0K (.82c) and 1200.0K (.83c) (LANL, 2011). Each material was run with the appropriate cross section added to the ZAID number, as well as a TMP card to individual cells. Input tests included all materials being at the same temperature except for the variable being actively investigated.

3.22. Pitch Variation

The distance between rods in the array by using engineering judgement and historical proportions for setting how far apart rods were in the reactor core. A sensitivity study was completed with rods beginning at 12cm apart, then 12.4 and 11.6cm apart to analyze which distance had the highest impact on criticality. Three input files were created with these cases and the 12cm apart case was chosen as the most critical. These input files are in Appendix C.

3.23. Moderator Variation

Three different moderators, air, water, and sodium were chosen to be tested as different moderators running through the steel pipes. Material 3 has its elemental composition and density changed to correctly match the moderator selection. These materials were each ran at the complete range of temperatures for both fuel and moderator. Once these cases were run, all critical cases were taken and analyzed for burnup measurements.

3.24. Size Variation

Upon completion of the base file, the entire reactor was both increased and decreased by a scale factor to analyze if overall size impacts criticality. While the original size is influenced by conceptual designs, increasing and decreasing the reactor in size up to a factor of two is acceptable (Beneš, 2021). This is due to the core still being able to fit within a 40-foot shipping container for transport, not taking away from the flexibility microreactors offer. The criticality values decreased with values evaluated at .75x, 1.5x, and 2x the original size all becoming subcritical, which can be seen in the size comparison table in Appendix D. Cases were also run given smaller/larger individual fuel rod sizes to ensure criticality would increase as expected. This was the case, with smaller and larger rods having delta K values of over 0.25 (Appendix D).

3.25. Power Variation

The base design was selected to run at a value of 5 MW based on realistic expectations of current concept designs. A sensitivity study was conducted to also include 2.5MW and 7MW power levels, outputs well within the range of what is considered a microreactor (Beneš, 2021). This value was changed within the burn card options. These values are for MWe and are run at full capacity throughout the year. All critical cases are run at these three power levels, both with and without control rods.

3.26. Control Rod Variation

While base cases were initially run without control rods inserted, testing was completed to ensure that cases would become sub-critical when rods were inserted. Boron

carbide (B4C) rods were used for burn credit cases at both full and half insertion. This material has been well documented as a successful neutron poison in existing reactor designs (Sanders, 2001). Enriched boron carbide control rods were also examined in identical cases, with a delta K value of 0.01195 examined between the two control rod types. While non-enriched rods were successful in meeting subcriticality, these enriched rods will add a small bump (under 5%) in further lowering k_{eff} amounts (Appendix D).

3.3. Computational Data

Once the variation analysis was accomplished, and the input MCNP files were developed, the MCNP was used to generate the required output files so that information generated could be analyzed to compile information and investigate trends within the design.

3.31 Variations in Reactor Component Temperatures

To begin the analysis, three matrices were produced to investigate which moderator choice produced the highest k_{eff} . These results are shown in the tables below.

Table 3.1: Variations in Air Temperature for Criticality Analysis

Base Temp	Air Temp	k_{eff}	Base Temp	Air Temp	k_{eff}	Base Temp	Air Temp	k_{eff}	Base Temp	Air Temp	k_{eff}
K	K		K	K		K	K		K	K	
293.6	293.6	0.93284	293.6	600	0.93358	293.6	900	0.93418	293.6	1200	0.93396
600	293.6	0.97675	600	600	0.97813	600	900	0.9776	600	1200	0.97676
900	293.6	0.99901	900	600	0.99983	900	900	0.99928	900	1200	0.9987
1200	293.6	0.99752	1200	600	0.99991	1200	900	1.0012	1200	1200	1.00038

Table 3.1 reflects variations within the air moderated temperature. The base temp column represents the temperature of all other materials within the reactor at a steady temperature. This includes the fuel and its TRISO layers, the graphite moderator, and the support pipes for the system. The column is named base temp to define that only one variable is being altered at a time. Air temperature is then modified to run at each reactor condition to evaluate its impact on reactivity of the system. The moderator temperature is assumed to be uniform throughout the tube. Several cases reach criticality, especially as base temperature reaches 1200K. As temperature increases throughout the entire reactor, criticality consequently increases. As only air temperature increases, there is not a defined increase in k_{eff} values. This is seen in the base temp 293.6 conditions of the table, where k_{eff} only slightly increases across room temperature and 900k, then decreases at 1200k. It is only when the rest of the materials in the reactor have an increase in temperature that k_{eff} begins to increase. Based on these results, it can be concluded that air temperature has a minimal impact on criticality.

Table 3.2: Variations in Sodium Temperature for Criticality Analysis

Base Temp	Sodium Temp	k _{eff}	Base Temp	Sodium Temp	k _{eff}	Base Temp	Sodium Temp	k _{eff}	Base Temp	Sodium Temp	k _{eff}
K	K		K	K		K	K		K	K	
293.6	293.6	0.93301	293.6	600	0.93301	293.6	900	0.93327	293.6	1200	0.93355
600	293.6	0.97577	600	600	0.97562	600	900	0.97494	600	1200	0.97500
900	293.6	0.99686	900	600	0.99665	900	900	0.99646	900	1200	0.99799
1200	293.6	0.99752	1200	600	0.99771	1200	900	0.99962	1200	1200	0.99842

Table 3.2 reflects variations within the sodium moderated temperature. Like air, there is no set pattern of k_{eff} growth for temperature increases in sodium only. Overall k_{eff} values are also slightly lower than found in air cases, primarily due to sodium’s primary function being heat removal and not effectively slowing down fast neutrons (Knief, 2003).

Table 3.3: Variations in Water Temperature for Criticality Analysis

Base Temp	Water Temp	k _{eff}	Base Temp	Water Temp	k _{eff}	Base Temp	Water Temp	k _{eff}	Base Temp	Water Temp	k _{eff}
K	K		K	K		K	K		K	K	
293.6	293.6	0.90288	293.6	600	0.91464	293.6	900	0.93212	293.6	1200	0.93326
600	293.6	0.94068	600	600	0.95371	600	900	0.97257	600	1200	0.97461
900	293.6	0.95634	900	600	0.97144	900	900	0.9943	900	1200	0.9958
1200	293.6	0.95362	1200	600	0.96828	1200	900	0.99431	1200	1200	0.99586

Table 3.3 reflects variations within the water moderated temperature. Unlike the other values, there is a small steady growth in k_{eff} for increases of temperature in water only. This is due to water turning to steam at higher temperatures and having a lower density. In this state,

water is less absorbent of neutrons and only graphite is left to effectively moderate. The thermal utilization factor is increased in the four-factor formula as the number of thermal neutrons is reduced, thus increasing reactivity. Overall k_{eff} values are also lower than found in air and sodium cases, not reaching desired quantities given the current layout. From here, the highest critical material, air, was selected as the moderator for design. A temperature study was then completed with changes to graphite and fuel individually.

Table 3.4: Variations in Graphite Temperature for Criticality Analysis

Base Temp	Graphite Temp	k_{eff}	Base Temp	Graphite Temp	k_{eff}	Base Temp	Graphite Temp	k_{eff}	Base Temp	Graphite Temp	k_{eff}
K	K		K	K		K	K		K	K	
293.6	293.6	0.93284	293.6	600	0.96618	293.6	900	0.99617	293.6	1200	1.00822
600	293.6	0.95033	600	600	0.97813	600	900	1.00506	600	1200	1.0159
900	293.6	0.94648	900	600	0.97129	900	900	0.99826	900	1200	1.009
1200	293.6	0.93935	1200	600	0.96278	1200	900	0.98809	1200	1200	1.001

Table 3.4 reflects variations within the graphite moderated temperature. A steady increase in k_{eff} value is seen as the graphite increases in temperature. In this core configuration, graphite has a positive temperature reactivity coefficient. F4 tallies were investigated in room temperature and 1200k graphite temperatures to compare neutron cross section behavior changes in graphite. The biggest difference between the two files was in the absorption cross sections. Room temperature graphite had an absorption cross section of 2.76457E-02 barns, while 1200k graphite had 1.75478E-02 barns, a significant 1.0098E-02 difference. For elastic scattering cross sections, values did not drastically change, with 6.87468E+01 barns for room temperature and

6.66188E+01barns at 1200k. The graphite has a reduced absorption cross section for thermal neutrons while the scattering cross section does not exhibit significant change with temperature. For thermal neutrons, the absorption cross section decreases as the neutron’s velocity increases (JANIS, 2024). This increase in temperature results in a positive temperature coefficient within graphite (Foulon, 1970). With a smaller absorption rate, neutrons can travel further within graphite without interaction and can escape outside of graphite to reach other fuel rods and increase fission. As the sum of coefficients corresponding to reactor temperatures sums to a positive global temperature coefficient, heating up graphite increases the resonance escape probability ρ in the four-factor formula and thus increases criticality. For current reactor design, this positive coefficient is beneficial as reactivity is just beginning to reach critical levels at the highest tested temperatures. However, increased temperatures above 1200K will continue to increase in criticality and require control rod manipulation to remain at steady state. This can be a sign of over moderation, whereas the positive temperature coefficient of the graphite moderator overrides the negative temperature feedback mechanisms exhibited by the fuel. Several high temperature values are in or near critical conditions and are deemed qualified for burnup calculations.

Table 3.5: Variations in Fuel Temperature for Criticality Analysis

Base Temp K	Fuel Temp K	k_{eff}	Base Temp K	Fuel Temp K	k_{eff}	Base Temp K	Fuel Temp K	k_{eff}	Base Temp K	Fuel Temp K	k_{eff}
293.6	293.6	0.93284	293.6	600	0.94896	293.6	900	0.94451	293.6	1200	0.93631
600	293.6	0.96718	600	600	0.97701	600	900	0.97105	600	1200	0.96036
900	293.6	0.99937	900	600	1.00697	900	900	0.99826	900	1200	0.98886
1200	293.6	1.01226	1200	600	1.01804	1200	900	1.0109	1200	1200	1.00097

Table 3.5 reflects variations within the fuel temperature. For this calculation, both the UO₂ and TRISO layers have been set to the related fuel temperature. A steady increase in k_{eff} value is seen only as the overall materials increase in temperature, not the fuel itself. This is a sign that the negative temperature coefficient of the fuel is working properly to lower the resonance escape probability ρ and working to bring down the overall global coefficient being raised by the graphite. This is displayed through the absorption cross section increasing across fuel temperatures, as produced by tally results. Room temperature fuel had absorption cross sections of 8.99724E-02 barns, while 1200k kelvin cases had an increase to 9.17302E-02 barns. This further points to the graphite temperature as a major factor in determining criticality, where reactivity will decrease as a function of fuel temperature. Several high material temperature values are at or near critical conditions and are deemed qualified for burnup calculations. Tally results are included in Appendix E.

3.32 Burnup Calculation Analysis

From variation tests, the highest criticality values were taken to run with burn cards at different operating powers, temperatures, and with control rods. Selection for cases included assuring cases could be sustained at temperatures presented in the table for years and not just snapshot cases, as stated by assumption eight. Burnup results are shown in the following graphs and tables representing this data are found in Appendix D. Error bars are included with ± 0.003 uncertainty for all results.

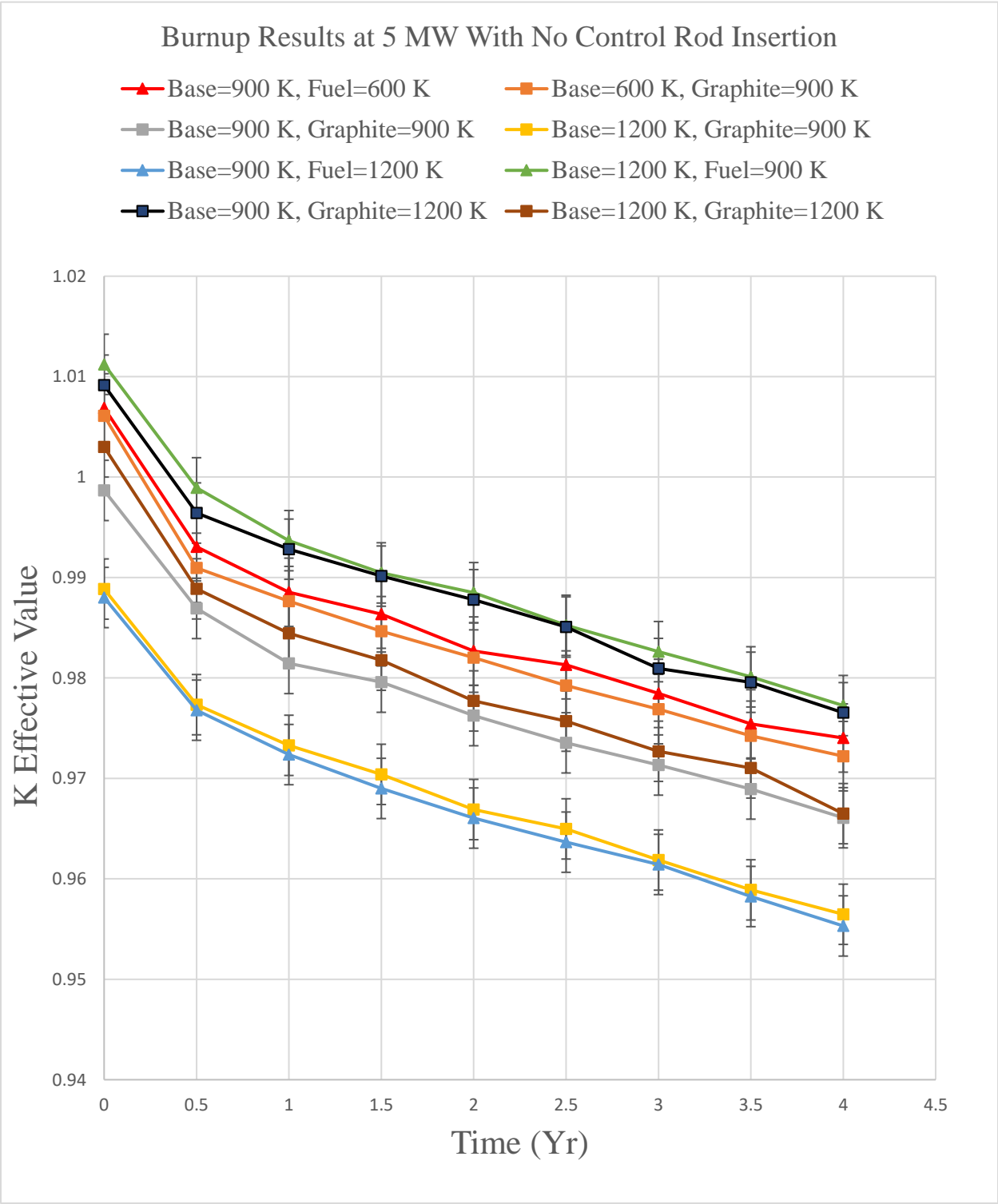


Figure 3.1: Burnup Results at 5 MW With No Control Rod Insertion

Figure 3.1 illustrates both the individual fuel and graphite contributions to criticality over time at 5 megawatts. Over time, the k_{eff} values drop as anticipated across all tests, with overall cases never increasing after initial startup. The sharpest decline for all conditions was during the first 180 days of operation in which the highest quantity of fresh fuel was available to burn. Slopes remained consistent across all scenarios, a good sign that burnup rates are also consistent. It can be observed that cases appear to run in similar pairs, such as the yellow and blue cases. The only difference between the two lines is whether the graphite or fuel was run warmer than the rest of the materials. Materials such as the steel pipes, the central zirconium hydride, and surrounding moderator temperatures included in the “base” temperatures also contribute to the small differences in k_{eff} values across tests. Data was deemed statistically different, with trends observed outside of the 1 sigma range.

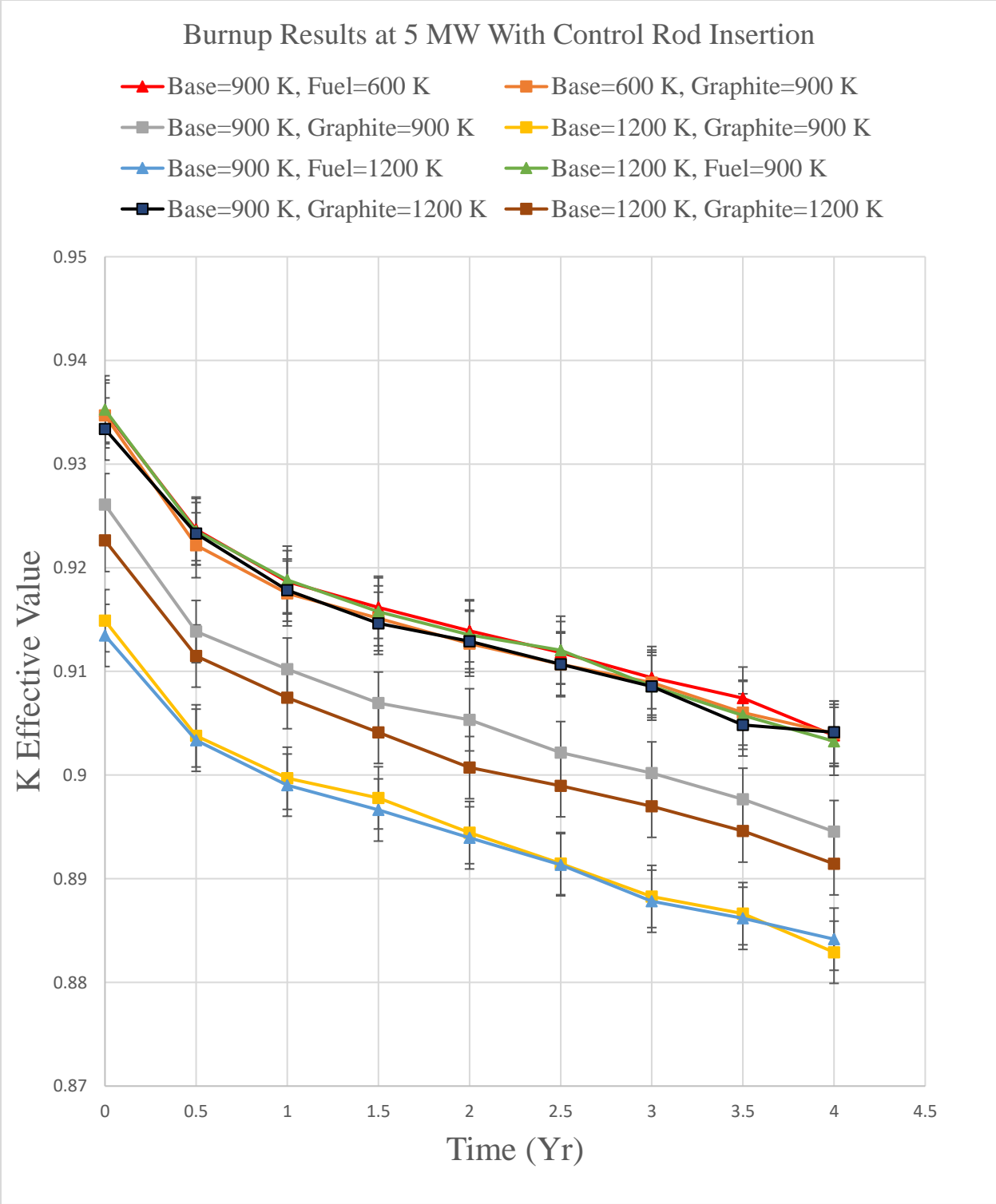


Figure 3.2: Burnup Results at 5 MW With Control Rod Insertion

Figure 3.2 illustrates both the individual fuel and graphite contributions to criticality over time at 5 megawatts with control rods fully inserted. Over time, the k_{eff} values drop as anticipated across all tests. The sharpest decline for all conditions was again during the first 180 days of operation in which the highest amount of energy was extracted per mass of initial fuel loaded. For this test condition, the fuel at 1200k and graphite at 900k cases are closely grouped together. These cases again feature similar qualities across graphite and fuel tests and although some slopes cross, data remains very close and consistent and should not be cause for concern in unexpected behavior. Data was deemed statistically different, with trends observed outside of the 1 sigma range.

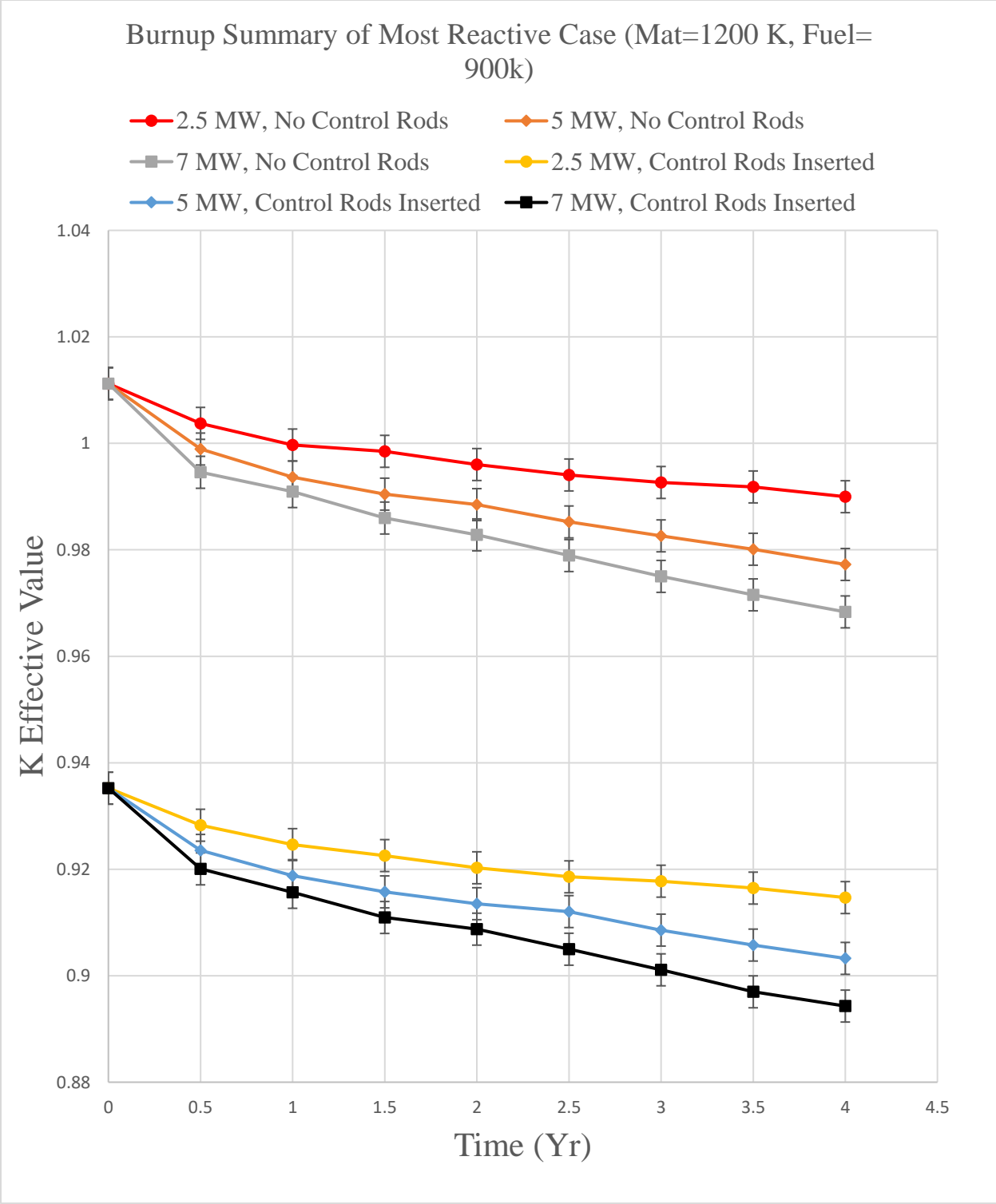


Figure 3.3: Burnup Summary of Most Reactive Case (Mat=1200 K, Fuel= 900k)

Figure 3.3 takes only one input file and includes its performance against all six burnup conditions. All power levels begin with the same k_{eff} , confirming that all cases start with the same criticality and different power levels over time should cause differences in k_{eff} values. This is also the case for non-control rod cases. All cases show properly that different levels of power will cause different rates of burnup, 7MW conditions having the largest delta k_{eff} . The percentages of fissions caused by neutrons remains relatively the same across cases, with most of the drop in k_{eff} coming from the reproduction factor η term in the four-factor equation. As fuel produces fission products as measured by the burn card, new fission products take up space in the fuel and thus decrease the number of neutrons produced compared to the number absorbed. The drop in k_{eff} from non-control rod cases to control rod cases occurs due to a decrease in neutron utilization f , rapidly increasing the number of neutrons absorbed. This gives further confidence that control rods properly satisfy the requirement to make the system subcritical when needed.

The percentages of fissions caused by neutrons in the thermal, intermediate, and fast neutron ranges were also examined across tables 3.1 to 3.4. Results in table 3.6 show that there was no substantial increase in the number of thermal neutrons created between temperature extremes, with less than 1% difference occurring across all materials.

. Table 3.6: Spectrum Percentage for Neutron Fission

Moderator (T=293.6K)	Base Temp (k)	Thermal	Intermediate	Fast
Air Temp	293.6	91.14%	6.33%	2.53%
Air Temp	1200	91.13%	6.34%	2.53%
Sodium Temp	293.6	91.13%	6.33%	2.54%
Sodium Temp	1200	91.15%	6.31%	2.54%
Water Temp	293.6	91.06%	6.32%	2.61%
Water Temp	1200	91.17%	6.24%	2.58%
Graphite Temp	293.6	91.14%	6.33%	2.53%
Graphite Temp	1200	91.75%	5.90%	2.36%

3.4. Data Analysis

Several key takeaways are developed from the data. Manipulation of individual components successfully signifies what contributes to criticality. As the temperature of the three coolant methods was altered, it is shown that these are not the driving force in the increase or decrease in reactivity. This can be attributed to the fact that these materials were only found in small quantities, flowing through pipes for cooling. It was only when the graphite moderator increased in temperature that k_{eff} increased. Graphite is considered the most vital component to the reactor's overall temperature, as increase in temperature increases criticality due to a high moderator to fuel ratio. This impacts the four-factor formula with an increase in resonance escape probability due to the graphite effectively absorbing less neutrons and a small increase in scattering cross sections. This guides the changing of k_{eff} across different temperatures at a fresh fuel state. As for burnup cases, consistent decrease in k_{eff} was seen across all material subsets. This was primarily due to the reproduction factor η slightly decreasing over the lifetime of the fuel, as the amount of fissionable U-235 is steadily decreasing. Fast fission factor ϵ is most impacted by the ratio of fast neutrons produced by fissions at all energies to the number of fast

neutrons produced in thermal fission. This value does not change much over both burnup and fresh fuel cases, as the layout of the reactor remains the same. The likelihood that the first collision of a fast neutron will be with a moderator remains the same.

When examining the percentages of fissions caused by neutrons, the spectrum of born neutrons between the fast, intermediate, and thermal range does not shift substantially between different temperatures (less than 1%). This suggests that materials consistently produce the same spectrum over time, adding little change to criticality. The thermal region is where the neutron absorption cross section is inversely proportional to neutron velocity, also known as $1/v$. This is shown in Figure 4.1, highlighting the resonances that neutrons must travel through to reach the thermal fissionable region.

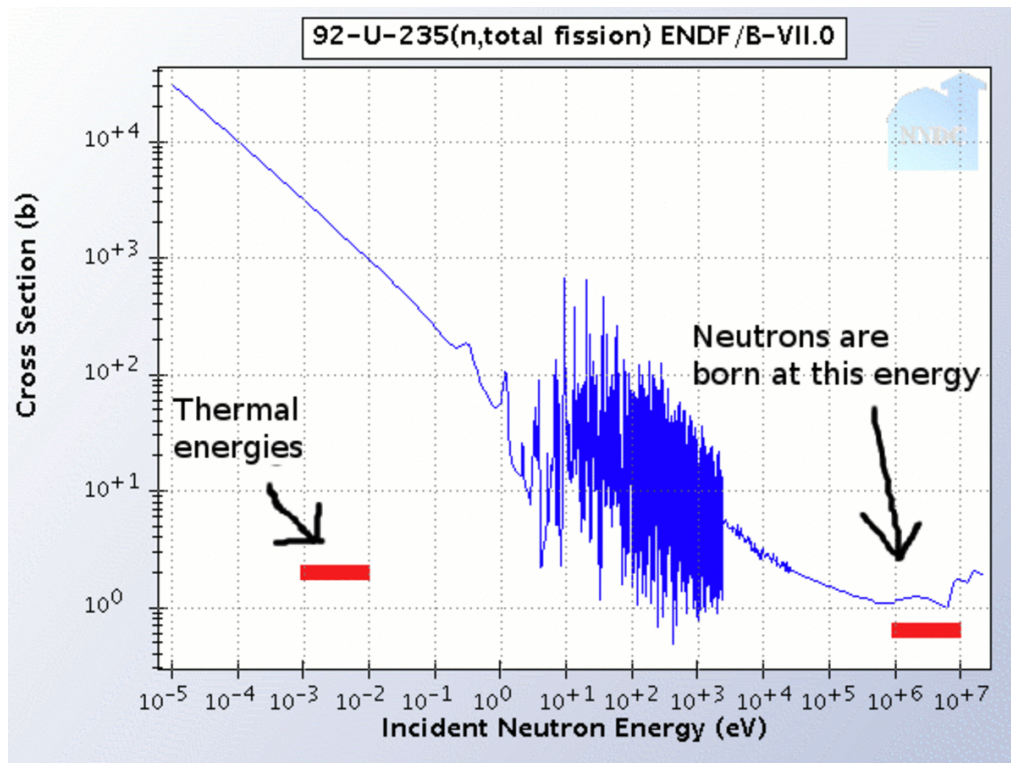


Figure 3.4: Neutron Reaction Probabilities in Uranium and Graphite (Touran,2023)

Data supports that resonance plays a large role in the ability of neutrons to travel to the thermal region, with approximately 90% of all fissions occurring in this region. Although U-235 has these resonances expanded as temperature increases, the high moderator to fuel ratio outweighs U-235's negative reactivity temperature coefficient. In graphite, neutrons manage to avoid absorption and thus are able to fission in this thermal range.

. Smaller amounts of fissile material due to burnup contribute as the primary cause for the decrease in reactivity. The data indicates that these configurations of microreactors can reach criticality, can be properly brought to subcritical levels if needed, and can last for lifespans expected by current designs.

Chapter 4. Conclusion

4.1. Conclusion

This thesis demonstrates how changing several different key elements to potential microreactor core designs will affect criticality. Input card designs were successfully reported in matrices format, with appropriate results showcasing different successful combinations of variables. The objectives of this thesis were met in several different capacities. Criticality control given reactivity feedback mechanisms and control rod insertion was properly demonstrated via control rod cases, dropping k_{eff} values across the full range of tests. As graphite had a positive temperature coefficient due to being over moderated, lowering the moderator to fuel ratio would decrease the reliance on graphite temperature and bring an overall negative temperature coefficient to the reactor as an added criticality safety feature. Data was found to be statistically different, with examined burnup uncertainties being outside of the 1 sigma range between all data points, marking a trend in data. Burnup was properly measured across several years, showing that operating a reactor at different output levels will increase burnup measurements. Sensitivity to temperature was investigated, with graphite having the largest impact on criticality when undergoing temperature change. While a wide temperature range was examined in the core, the 900K fuel temperature levels proved to yield the best reactions when combined with a 1200K graphite temperature. While the most reactive, this configuration still successfully dropped under subcritical levels to demonstrate controllability. With control rods half inserted, criticality slightly lowered to a value very close to 1, showing proper reactions to control rod manipulation for control. Overall, this thesis yielded findings consistent with current market designs, conceptual ideas, and further confirmed the ability to control a nuclear reaction on a much smaller scale than current US power plants.

4.2. Suggested Future Work

The base input file is set up so that several materials can be run through the coolant pipes with a simple material switch. This makes it easy for designers to go through and select any material desired, especially given the MCNP Manual Appendix G. Other variables are easily manipulated as well to meet design requirements for plants with similar layouts. The layout of the reactor can be manipulated to increase the physical amount of fuel present and remove graphite, thus decreasing the moderator to fuel ratio and introducing a global negative reactor temperature coefficient. Dose calculations can also be created using the existing geometry, considering assumption six be removed for a specific plant design. The created matrices can continuously be added to and potentially used to create an official guideline document for microreactor neutronics cases.

While the cases produced come with high confidence levels in results, several actions can be taken to expand on this research and build a more comprehensive reactor. One key component missing is computational fluid dynamic analysis. This computationally expensive and complex analysis is outside of the scope of this thesis. In a reactor company, a neutronics engineer would submit their input files to a CFD engineer for analysis, outsourcing the work to an entirely different department. If a CFD analysis were to be done, the model would have a temperature gradient across all materials representative of a real heat transfer case. To offset this, cases were run with best engineering judgement of fuel temperature and limited information regarding current microreactor heat transfer information.

Appendix A: Density Homogenization Calculations

Appendix A provides the calculations used to find the material density used in the homogenous TRISO layers.

Table A.1: Material Density Calculations

Material	Density(g/cc)	Thickness(um)	Volume (mm ³)	Percentage of Total volume	Buffer Density Average(g/cc)	Percentage of Buffer Layers
UO ₂	10.96	800	0.268082573	27.10%	2.577128814	
Buffer (Carbon)	0.98	75	0.180837927	14.23%		19.52%
Inner PyC Coating	1.85	35	0.106726709	8.40%		11.52%
SiC coating	3.2	36.7	0.128793497	10.14%		13.90%
Outer PyC coating	1.86	20	0.077898485	6.13%		8.41%
NITE SiC Matrix	3.2	30% of the overall space.	0.508226	34%		46.64%

Table A.2: Material Card Percentages

Material Card 2 Weight Fraction						Totals:	Percentage of MT Card
0.06	U-235	0.152037	O-16	0.788	U-238	C-12	45.73485
19.524	C-12					H-1	6.03016
0.639	H-1	8.708	C-12	2.178	O-16	S-14	44.48094
9.733	S-14	4.171	C-12			O-16	3.480774
5.887	H-1	0.636	C-12	1.590	O-16		
32.647	S-14	13.992	C-12				

Appendix B: Upper Safety Limit Development

Appendix B includes the different input files run to evaluate the upper safety limit for the MCNP download. The results for 293.6k base case are listed below. Cases including sodium and water moderators are included in the OUTPUT.ZIP file.

Benchmark population = 127
Population weight = 44.32953
Maximum similarity = 0.80673

Bias = 0.00953
Bias uncertainty = 0.00713
Nuc Data uncert margin = 0.00233
Software/method margin = 0.00500
Non-coverage penalty = 0.00000

benchmark	ck	weight
heu-sol-therm-042-006.i	0.8067	1.0000
heu-sol-therm-042-004.i	0.8059	0.9953
heu-sol-therm-042-005.i	0.8056	0.9936
heu-sol-therm-042-007.i	0.8047	0.9888
heu-sol-therm-032-001.i	0.8022	0.9745
heu-sol-therm-042-003.i	0.8019	0.9726
heu-sol-therm-042-008.i	0.8001	0.9623
leu-sol-therm-020-004.i	0.7792	0.8440
heu-sol-therm-042-002.i	0.7791	0.8438
leu-sol-therm-021-004.i	0.7739	0.8144
heu-sol-therm-042-001.i	0.7736	0.8124
leu-sol-therm-020-003.i	0.7642	0.7596
leu-sol-therm-002-001.i	0.7588	0.7289
leu-sol-therm-021-003.i	0.7585	0.7273
leu-sol-therm-020-002.i	0.7442	0.6463
leu-sol-therm-004-007.i	0.7420	0.6339
leu-sol-therm-021-002.i	0.7380	0.6114
leu-comp-therm-007-004.i	0.7371	0.6064
leu-sol-therm-004-006.i	0.7339	0.5882
heu-comp-therm-002-010.i	0.7311	0.5721
leu-sol-therm-020-001.i	0.7305	0.5689
leu-sol-therm-002-002.i	0.7291	0.5609
leu-sol-therm-004-005.i	0.7247	0.5357
heu-sol-therm-043-003.i	0.7226	0.5239
heu-sol-therm-013-002.i	0.7224	0.5232
heu-sol-therm-013-004.i	0.7200	0.5095
leu-sol-therm-021-001.i	0.7197	0.5077
heu-sol-therm-013-001.i	0.7194	0.5060
heu-sol-therm-013-003.i	0.7188	0.5029

leu-sol-therm-007-049.i	0.7159	0.4861
leu-sol-therm-007-005.i	0.7143	0.4771
leu-sol-therm-004-004.i	0.7133	0.4718
leu-comp-therm-005-004.i	0.7107	0.4570
leu-comp-therm-011-015.i	0.7093	0.4490
leu-sol-therm-007-004.i	0.7057	0.4287
leu-sol-therm-007-036.i	0.7051	0.4250
leu-comp-therm-011-007.i	0.7043	0.4207
leu-comp-therm-011-003.i	0.7034	0.4156
heu-sol-therm-012-001.i	0.7027	0.4113
leu-comp-therm-005-003.i	0.7010	0.4017
leu-comp-therm-060-005.i	0.7008	0.4007
leu-sol-therm-004-003.i	0.7004	0.3984
heu-comp-therm-002-009.i	0.7000	0.3963
leu-comp-therm-010-005.i	0.6972	0.3803
leu-comp-therm-011-009.i	0.6954	0.3700
leu-comp-therm-010-006.i	0.6942	0.3635
leu-comp-therm-028-017.i	0.6937	0.3604
leu-comp-therm-022-007.i	0.6927	0.3550
leu-comp-therm-017-004.i	0.6917	0.3493
leu-comp-therm-017-008.i	0.6916	0.3487
leu-sol-therm-007-032.i	0.6904	0.3421
leu-comp-therm-008-008.i	0.6894	0.3365
leu-sol-therm-004-002.i	0.6893	0.3360
leu-comp-therm-017-006.i	0.6883	0.3300
leu-comp-therm-008-007.i	0.6874	0.3248
leu-comp-therm-022-006.i	0.6867	0.3212
leu-comp-therm-017-007.i	0.6864	0.3193
leu-comp-therm-017-010.i	0.6861	0.3178
leu-comp-therm-008-002.i	0.6860	0.3172
leu-comp-therm-008-005.i	0.6858	0.3158
leu-comp-therm-017-005.i	0.6844	0.3082
leu-comp-therm-010-008.i	0.6843	0.3076
leu-comp-therm-060-003.i	0.6840	0.3057
leu-comp-therm-028-020.i	0.6839	0.3052
leu-comp-therm-008-011.i	0.6825	0.2975
leu-comp-therm-028-018.i	0.6822	0.2955
leu-comp-therm-017-014.i	0.6810	0.2887
leu-comp-therm-017-011.i	0.6792	0.2786
leu-comp-therm-017-013.i	0.6792	0.2785
heu-sol-therm-025-008.i	0.6786	0.2750
leu-comp-therm-017-012.i	0.6784	0.2742
leu-comp-therm-011-002.i	0.6784	0.2741
leu-comp-therm-010-007.i	0.6780	0.2720
leu-sol-therm-007-030.i	0.6775	0.2689
leu-sol-therm-004-001.i	0.6758	0.2593

heu-sol-therm-025-006.i	0.6752	0.2558
leu-sol-therm-007-002.i	0.6740	0.2490
leu-comp-therm-060-001.i	0.6732	0.2448
leu-comp-therm-017-003.i	0.6729	0.2433
leu-comp-therm-017-009.i	0.6727	0.2419
heu-sol-therm-025-013.i	0.6725	0.2407
leu-comp-therm-008-001.i	0.6705	0.2292
ieu-comp-therm-002-003.i	0.6701	0.2269
leu-comp-therm-028-019.i	0.6698	0.2256
leu-comp-therm-001-007.i	0.6691	0.2215
leu-comp-therm-001-005.i	0.6690	0.2212
leu-comp-therm-017-002.i	0.6690	0.2212
leu-comp-therm-010-011.i	0.6681	0.2157
leu-comp-therm-001-008.i	0.6678	0.2140
heu-comp-therm-002-008.i	0.6669	0.2092
leu-comp-therm-017-001.i	0.6666	0.2072
leu-comp-therm-010-009.i	0.6664	0.2062
leu-comp-therm-010-012.i	0.6662	0.2050
leu-comp-therm-028-016.i	0.6658	0.2028
leu-comp-therm-010-010.i	0.6638	0.1916
heu-sol-therm-025-007.i	0.6625	0.1843
leu-comp-therm-001-006.i	0.6624	0.1836
leu-comp-therm-001-003.i	0.6619	0.1805
leu-sol-therm-007-014.i	0.6605	0.1726
leu-comp-therm-010-013.i	0.6601	0.1704
leu-comp-therm-001-004.i	0.6587	0.1626
heu-sol-therm-043-002.i	0.6585	0.1613
leu-comp-therm-007-007.i	0.6530	0.1302
leu-comp-therm-001-002.i	0.6527	0.1290
leu-comp-therm-007-010.i	0.6517	0.1229
leu-comp-therm-028-015.i	0.6500	0.1134
heu-sol-therm-025-015.i	0.6499	0.1129
heu-sol-therm-025-011.i	0.6480	0.1020
heu-sol-therm-025-012.i	0.6471	0.0971
leu-comp-therm-028-014.i	0.6468	0.0951
heu-sol-therm-025-018.i	0.6467	0.0946
leu-comp-therm-028-012.i	0.6461	0.0912
leu-comp-therm-010-004.i	0.6457	0.0893
leu-comp-therm-010-003.i	0.6427	0.0724
heu-sol-therm-025-014.i	0.6422	0.0693
leu-comp-therm-001-001.i	0.6420	0.0683
leu-comp-therm-060-006.i	0.6401	0.0575
leu-comp-therm-002-005.i	0.6395	0.0542
leu-comp-therm-010-001.i	0.6383	0.0471
heu-comp-therm-002-007.i	0.6381	0.0461
heu-sol-therm-025-017.i	0.6368	0.0385

leu-comp-therm-010-002.i	0.6350	0.0287
leu-comp-therm-009-007.i	0.6340	0.0230
heu-sol-therm-025-009.i	0.6327	0.0154
leu-comp-therm-009-023.i	0.6313	0.0079
leu-comp-therm-060-004.i	0.6305	0.0033
leu-comp-therm-009-016.i	0.6300	0.0006

USL Summary Table

application	calc margin	data unc (1-sigma)	baseline USL	k(calc) > USL
job1.i	0.01666	0.00233	0.97228	-0.03722

Appendix C: Input Files

Appendix C includes the different input files run to evaluate the full range of conditions the microreactor could face. Included in this Appendix are 3 cases each with a different moderator as well as 2 burn card cases: one with and one without control rods. The full list of input files can be found in the INPUT.ZIP file.

MICROREACTOR WITH AIR MODERATOR

C

C ~~~~~ CELL CARD

```
~~~~~
C Cylinder Pin 1, the Fully Ceramic Micro-Encapsulated Fuel
1 1 -10.96 -1 u=1 tmp=5.1702E-08 imp:n=1 $UO2 without the TRISO
components, universe 1 (T=600k)
2 2 -2.577 1 -2 u=1 tmp=5.1702E-08 imp:n=1 $TRISO shielding components,
universe 1 (T=600k)
3 6 -1.70 2 u=1 tmp=5.1702E-08 imp:n=1 $outside of layer (T=600k)
C Cylinder 2 air cooled system
4 3 -0.001293 -3 u=2 tmp=5.1702E-08 imp:n=1 $air flow, universe 2 (T=600k)
5 4 -8 3 -4 u=2 tmp=5.1702E-08 imp:n=1 $Steel pipe, universe 2 (T=600k)
6 6 -1.70 4 u=2 tmp=5.1702E-08 imp:n=1 $outside of layer (T=600k)
C Center movement device
7 5 -5.61 -5 u=3 tmp=5.1702E-08 imp:n=1 $Zirconium Hydride, Universe 3
(T=600k)
8 4 -8 5 -6 u=3 tmp=5.1702E-08 imp:n=1 $Steel pipe, universe 3 (T=600k)
9 6 -1.70 6 u=3 tmp=5.1702E-08 imp:n=1 $outside of layer(T=600k)
c -----
10 7 -2.25 -7 8 -9 10 u=4 imp:n=1 lat=1 fill=-9:9 -9:9 0:0 $square lattice-cell
4 4 4 4 4 4 4 4 4 4 4 4 4 4 4 4 4 4 4 4 4 4
4 4 4 4 4 4 4 4 4 4 4 4 4 4 4 4 4 4 4 4 4 4
4 4 4 4 4 4 4 4 4 4 4 4 4 4 4 4 4 4 4 4 4 4
4 4 4 1 1 1 1 1 1 1 1 1 1 1 1 1 1 1 1 4 4 4
4 4 4 1 1 1 1 1 1 1 1 1 1 1 1 1 1 1 1 4 4 4
4 4 4 1 1 2 1 1 1 1 1 1 1 1 2 1 1 1 1 4 4 4
4 4 4 1 1 1 1 1 1 1 1 1 1 1 1 1 1 1 1 4 4 4
4 4 4 1 1 1 1 2 1 1 1 2 1 1 1 1 1 1 1 4 4 4
4 4 4 1 1 1 1 1 1 1 1 1 1 1 1 1 1 1 1 4 4 4
4 4 4 1 1 1 1 1 1 1 1 1 1 1 1 1 1 1 1 4 4 4
4 4 4 1 1 1 1 2 1 1 1 2 1 1 1 1 1 1 1 4 4 4
4 4 4 1 1 1 1 1 1 1 1 1 1 1 1 1 1 1 1 4 4 4
4 4 4 1 1 2 1 1 1 1 1 1 1 1 2 1 1 1 1 4 4 4
4 4 4 1 1 1 1 1 1 1 1 1 1 1 1 1 1 1 1 4 4 4
4 4 4 1 1 1 1 1 1 1 1 1 1 1 1 1 1 1 1 4 4 4
4 4 4 4 4 4 4 4 4 4 4 4 4 4 4 4 4 4 4 4 4 4
```

```

4 4 4 4 4 4 4 4 4 4 4 4 4 4 4 4 4 4 4 4
4 4 4 4 4 4 4 4 4 4 4 4 4 4 4 4 4 4 4 4
11 6 -1.70 -11 12 -13 14 17 -18 imp:n=1 fill=4 tmp=5.1702E-08 $square assembly
12 7 -2.25 -11 12 -13 14 -15 80 imp:n=1 $bottom concrete
13 7 -2.25 -11 12 -13 14 16 -90 imp:n=1 Stop concrete
14 6 -1.70 -11 12 -13 14 15 -17 imp:n=1 tmp=5.1702E-08 $bottom moderator
15 6 -1.70 -11 12 -13 14 18 -16 imp:n=1 tmp=5.1702E-08 Stop moderator
16 0 11:-12:13:-14:-80:90 imp:n=0 $Outside World

```

C Line above is blank delimiter.

C ~~~~~ SURFACE CARD

```

~~~~~
1 cz 0.55 $cm inner cylinder of UO2
2 cz 1.95 $cm outer layer of fcm pellet
3 cz 3 $cm inner cylinder of the moderator
4 cz 4 $cm layer of aluminum pipe
5 cz 3 $cm inner layer of the ZrH
6 cz 4 $cm outer layer of the ZrH
7 px 6.0 $1st side of the square lattice
8 px -6.0 $2nd side of the square lattice
9 py 6.0 $3rd side of the square lattice
10 py -6.0 $4th side of the square lattice
11 px 110.3 $1st side of the square assembly
12 px -110.3 $2nd side of the square assembly
13 py 110.3 $3rd side of the square assembly
14 py -110.3 $4th side of the square assembly
15 pz -210 $bottom of conc
16 pz 210 $top of conc
17 pz -200 $bottom of reflector
18 pz 200 $top of reflector
80 pz -230 $bottom of reflector
90 pz 230 $top of reflector

```

C Line above is blank delimiter.

C ~~~~~ MATERIAL CARD

```

~~~~~
C (Material#) (Fraction + Atomic - Weight) (include sources)
C Material entries must start in the column 6
C BURN TIME= 365 365 365 365 365 365 MAT = 1 Power =5.0
C BOPT=1.0 11 1 OMIT=1,8,6014,7016,8018,9018,13026,13028,14027,16031
C MPHYS ON
m1 92235.81c 0.202 $Uranium 235 inside fuel kernel rho=10.96 g/cm^3,20%
8016.81c 2.0 $Oxygen inside fuel kernel+PyC
92238.81c 0.798 $Uranium 238 inside fuel kernel
mt1 o2-u.23t $material card
m2 6000.81c -0.45735 $Carbon Buffer layers 45.735 rho=0.98 g/cm^3

```


C ~~~~~ CELL CARD

```
~~~~~
C Cylinder Pin 1, the Fully Ceramic Micro-Encapsulated Fuel
1 1 -10.96 -1 u=1 tmp=5.1702E-08 imp:n=1 $UO2 without the TRISO
components, universe 1 (T=600k)
2 2 -2.577 1 -2 u=1 tmp=5.1702E-08 imp:n=1 $TRISO shielding components,
universe 1 (T=600k)
3 6 -1.70 2 u=1 tmp=5.1702E-08 imp:n=1 $outside of layer (T=600k)
C Cylinder 2 air cooled system
4 3 -0.997 -3 u=2 tmp=5.1702E-08 imp:n=1 $water, universe 2 (T=600k)
5 4 -8 3 -4 u=2 tmp=5.1702E-08 imp:n=1 $Steel pipe, universe 2 (T=600k)
6 6 -1.70 4 u=2 tmp=5.1702E-08 imp:n=1 $outside of layer (T=600k)
C Center movement device
7 5 -5.61 -5 u=3 tmp=5.1702E-08 imp:n=1 $Zirconium Hydride, Universe 3
(T=600k)
8 4 -8 5 -6 u=3 tmp=5.1702E-08 imp:n=1 $Steel pipe, universe 3 (T=600k)
9 6 -1.70 6 u=3 tmp=5.1702E-08 imp:n=1 $outside of layer(T=600k)
c -----
10 7 -2.25 -7 8 -9 10 u=4 imp:n=1 lat=1 fill=-9:9 -9:9 0:0 $square lattice-cell
 4 4 4 4 4 4 4 4 4 4 4 4 4 4 4 4 4 4
 4 4 4 4 4 4 4 4 4 4 4 4 4 4 4 4 4 4
 4 4 4 4 4 4 4 4 4 4 4 4 4 4 4 4 4 4
 4 4 4 1 1 1 1 1 1 1 1 1 1 1 1 1 4 4 4
 4 4 4 1 1 1 1 1 1 1 1 1 1 1 1 1 4 4 4
 4 4 4 1 1 2 1 1 1 1 1 1 1 2 1 1 4 4 4
 4 4 4 1 1 1 1 1 1 1 1 1 1 1 1 1 4 4 4
 4 4 4 1 1 1 1 2 1 1 1 2 1 1 1 1 4 4 4
 4 4 4 1 1 1 1 1 1 1 1 1 1 1 1 1 4 4 4
 4 4 4 1 1 1 1 1 1 3 1 1 1 1 1 1 4 4 4
 4 4 4 1 1 1 1 1 1 1 1 1 1 1 1 1 4 4 4
 4 4 4 1 1 1 1 2 1 1 1 2 1 1 1 1 4 4 4
 4 4 4 1 1 1 1 1 1 1 1 1 1 1 1 1 4 4 4
 4 4 4 1 1 2 1 1 1 1 1 1 2 1 1 1 4 4 4
 4 4 4 1 1 1 1 1 1 1 1 1 1 1 1 1 4 4 4
 4 4 4 4 4 4 4 4 4 4 4 4 4 4 4 4 4 4
 4 4 4 4 4 4 4 4 4 4 4 4 4 4 4 4 4 4
 4 4 4 4 4 4 4 4 4 4 4 4 4 4 4 4 4 4
11 6 -1.70 -11 12 -13 14 17 -18 imp:n=1 fill=4 tmp=5.1702E-08 $square assembly
12 7 -2.25 -11 12 -13 14 -15 80 imp:n=1 $bottom concrete
13 7 -2.25 -11 12 -13 14 16 -90 imp:n=1 $top concrete
14 6 -1.70 -11 12 -13 14 15 -17 imp:n=1 tmp=5.1702E-08 $bottom moderator
15 6 -1.70 -11 12 -13 14 18 -16 imp:n=1 tmp=5.1702E-08 $top moderator
16 0 11:-12:13:-14:-80:90 imp:n=0 $Outside World
```

C Line above is blank delimiter.

C ~~~~~ SURFACE CARD

1 cz 0.55 \$cm inner cylinder of UO2
2 cz 1.95 \$cm outer layer of fcm pellet
3 cz 3 \$cm inner cylinder of the moderator
4 cz 4 \$cm layer of aluminum pipe
5 cz 3 \$cm inner layer of the ZrH
6 cz 4 \$cm outer layer of the ZrH
7 px 6.0 \$1st side of the square lattice
8 px -6.0 \$2nd side of the square lattice
9 py 6.0 \$3rd side of the square lattice
10 py -6.0 \$4th side of the square lattice
11 px 110.3 \$1st side of the square assembly
12 px -110.3 \$2nd side of the square assembly
13 py 110.3 \$3rd side of the square assembly
14 py -110.3 \$4th side of the square assembly
15 pz -210 \$bottom of conc
16 pz 210 \$top of conc
17 pz -200 \$bottom of reflector
18 pz 200 \$top of reflector
80 pz -230 \$bottom of reflector
90 pz 230 \$top of reflector

C Line above is blank delimiter.

C ~~~~~ MATERIAL CARD

C (Material#) (Fraction + Atomic - Weight) (include sources)
C Material entries must start in the column 6
C BURN TIME= 365 365 365 365 365 365 MAT = 1 Power =5.0
C BOPT=1.0 11 1 OMIT=1,8,6014,7016,8018,9018,13026,13028,14027,16031
C MPHYS ON
m1 92235.81c 0.202 \$Uranium 235 inside fuel kernel rho=10.96 g/cm^3,20%
8016.81c 2.0 \$Oxygen inside fuel kernel+PyC
92238.81c 0.798 \$Uranium 238 inside fuel kernel
mt1 o2-u.23t \$material card
m2 6000.81c -0.45735 \$Carbon Buffer layers 45.735 rho=0.98 g/cm^3
1001.81c -0.06030 \$Hydrogen from PyC 6.030
14028.81c -0.44481 \$Solid Silicon Carbide+Silicon Matrix rho=3.20g/cm^3
8016.81c -0.03754 \$Oxygen from PyC+SiC coatings
m3 1001.81c -0.112 8016.81c -0.888 \$water air rho=-0.997
m4 14028.81c -0.01
24050.81c -0.19
28058.81c -0.095
26054.81c -0.705 \$Steel, Stainless 304L rho=8 g/cm^3
m5 40090.81c -0.498
40091.81c -0.112

```

40092.81c -0.17
40094.81c -0.175
40096.81c -0.028
1001.81c -0.017 $Zirconium Hydride rho=5.61 g/cm^3
m6  6000.81c -1  $Graphite core rho=1.70 g/cc
mt6  grph.23t      $Change for different temperatures
m7  1001.80c -0.004529 $Concrete(Los Alamos (MCNP) Mix rho=2.25 g/cc
8016.80c -0.511670
14028.80c -0.360360
13027.80c -0.0355
11023.80c -0.015270
20040.80c -0.05791
26054.80c -0.013780
C ~ ~ ~ CRITICALITY CODE ~ ~ ~ ~ ~ ~ ~ ~ ~ ~ ~ ~ ~ ~ ~ ~ ~ ~ ~ ~ ~ ~
C
kcode 10000 1 150 800 $ KCODE (# of Neutrons/Cycle) (Initial keff guess) (# of skipped
cycles)(# of total cycles)
C # of Neutrons/Cycle Recommended 10^3 for simple geometries; 10^6 for complex
C Initial keff guess – Usually 1
C # of Skipped Cycles – 10% of Total Cycles
C # of Total Cycles – More cycles decreases error
ksrc -12 0 0 $ KSRC x y z x y z ...
print, end of card

MICROREACTOR CORE, SODIUM MODERATED
C
C ~~~~~ CELL CARD
~~~~~
C Cylinder Pin 1, the Fully Ceramic Micro-Encapsulated Fuel
1 1 -10.96 -1  u=1 tmp=5.1702E-08 imp:n=1 $UO2 without the TRISO
components, universe 1 (T=600k)
2 2 -2.577 1 -2  u=1 tmp=5.1702E-08 imp:n=1 $TRISO shielding components,
universe 1 (T=600k)
3 6 -1.70 2   u=1 tmp=5.1702E-08 imp:n=1 $outside of layer (T=600k)
C Cylinder 2 air cooled system
4 3 -0.971 -3  u=2 tmp=5.1702E-08 imp:n=1 $Sodium, universe 2 (T=600k)
5 4 -8 3 -4 u=2  tmp=5.1702E-08 imp:n=1 $Steel pipe, universe 2 (T=600k)
6 6 -1.70 4   u=2 tmp=5.1702E-08 imp:n=1 $outside of layer (T=600k)
C Center movement device
7 5 -5.61 -5   u=3 tmp=5.1702E-08 imp:n=1 $Zirconium Hydride, Universe 3
(T=600k)
8 4 -8 5 -6 u=3  tmp=5.1702E-08 imp:n=1 $Steel pipe, universe 3 (T=600k)
9 6 -1.70 6   u=3 tmp=5.1702E-08 imp:n=1 $outside of layer(T=600k)
c -----
10 7 -2.25 -7 8 -9 10 u=4 imp:n=1 lat=1 fill=-9:9 -9:9 0:0 $square lattice-cell
4 4 4 4 4 4 4 4 4 4 4 4 4 4 4 4

```

```

4 4 4 4 4 4 4 4 4 4 4 4 4 4 4 4 4 4 4 4 4
4 4 4 4 4 4 4 4 4 4 4 4 4 4 4 4 4 4 4 4 4
4 4 4 1 1 1 1 1 1 1 1 1 1 1 1 1 1 4 4 4
4 4 4 1 1 1 1 1 1 1 1 1 1 1 1 1 1 4 4 4
4 4 4 1 1 2 1 1 1 1 1 1 1 2 1 1 4 4 4
4 4 4 1 1 1 1 1 1 1 1 1 1 1 1 1 4 4 4
4 4 4 1 1 1 1 2 1 1 1 2 1 1 1 1 4 4 4
4 4 4 1 1 1 1 1 1 1 1 1 1 1 1 1 4 4 4
4 4 4 1 1 1 1 1 1 3 1 1 1 1 1 1 4 4 4
4 4 4 1 1 1 1 1 1 1 1 1 1 1 1 1 4 4 4
4 4 4 1 1 1 1 2 1 1 1 2 1 1 1 1 4 4 4
4 4 4 1 1 1 1 1 1 1 1 1 1 1 1 1 4 4 4
4 4 4 1 1 1 1 1 1 1 1 1 1 1 1 1 4 4 4
4 4 4 1 1 2 1 1 1 1 1 1 1 2 1 1 4 4 4
4 4 4 1 1 1 1 1 1 1 1 1 1 1 1 1 4 4 4
4 4 4 1 1 1 1 1 1 1 1 1 1 1 1 1 4 4 4
4 4 4 4 4 4 4 4 4 4 4 4 4 4 4 4 4 4 4 4 4
4 4 4 4 4 4 4 4 4 4 4 4 4 4 4 4 4 4 4 4 4
4 4 4 4 4 4 4 4 4 4 4 4 4 4 4 4 4 4 4 4 4
11 6 -1.70 -11 12 -13 14 17 -18 imp:n=1 fill=4 tmp=5.1702E-08 $square assembly
12 7 -2.25 -11 12 -13 14 -15 80 imp:n=1 $bottom concrete
13 7 -2.25 -11 12 -13 14 16 -90 imp:n=1 $top concrete
14 6 -1.70 -11 12 -13 14 15 -17 imp:n=1 tmp=5.1702E-08 $bottom moderator
15 6 -1.70 -11 12 -13 14 18 -16 imp:n=1 tmp=5.1702E-08 $top moderator
16 0 11:-12:13:-14:-80:90 imp:n=0 $Outside World

```

C Line above is blank delimiter.

C ~~~~~ SURFACE CARD

~~~~~

```

1 cz 0.55 $cm inner cylinder of UO2
2 cz 1.95 $cm outer layer of fcm pellet
3 cz 3 $cm inner cylinder of the moderator
4 cz 4 $cm layer of aluminum pipe
5 cz 3 $cm inner layer of the ZrH
6 cz 4 $cm outer layer of the ZrH
7 px 6.0 $1st side of the square lattice
8 px -6.0 $2nd side of the square lattice
9 py 6.0 $3rd side of the square lattice
10 py -6.0 $4th side of the square lattice
11 px 110.3 $1st side of the square assembly
12 px -110.3 $2nd side of the square assembly
13 py 110.3 $3rd side of the square assembly
14 py -110.3 $4th side of the square assembly
15 pz -210 $bottom of conc
16 pz 210 $top of conc
17 pz -200 $bottom of reflector
18 pz 200 $top of reflector

```

80 pz -230 \$bottom of reflector  
90 pz 230 \$top of reflector

C Line above is blank delimiter.  
C ~~~~~ MATERIAL CARD

~~~~~

C (Material#) (Fraction + Atomic - Weight) (include sources)
C Material entries must start in the column 6
C BURN TIME= 365 365 365 365 365 365 MAT = 1 Power =5.0
C BOPT=1.0 11 1 OMIT=1,8,6014,7016,8018,9018,13026,13028,14027,16031
C MPHYS ON

m1 92235.81c 0.202 \$Uranium 235 inside fuel kernel rho=10.96 g/cm³,20%
8016.81c 2.0 \$Oxygen inside fuel kernel+PyC
92238.81c 0.798 \$Uranium 238 inside fuel kernel

mt1 o2-u.23t \$material card

m2 6000.81c -0.45735 \$Carbon Buffer layers 45.735 rho=0.98 g/cm³
1001.81c -0.06030 \$Hydrogen from PyC 6.030
14028.81c -0.44481 \$Solid Silicon Carbide+Silicon Matrix rho=3.20g/cm³
8016.81c -0.03754 \$Oxygen from PyC+SiC coatings

m3 11022.81c -1 \$sodium 1 rho=-0.971

m4 14028.81c -0.01
24050.81c -0.19
28058.81c -0.095
26054.81c -0.705 \$Steel, Stainless 304L rho=8 g/cm³

m5 40090.81c -0.498
40091.81c -0.112
40092.81c -0.17
40094.81c -0.175
40096.81c -0.028
1001.81c -0.017 \$Zirconium Hydride rho=5.61 g/cm³

m6 6000.81c -1 \$Graphite core rho=1.70 g/cc

mt6 grph.23t \$Change for different temperatures

m7 1001.80c -0.004529 \$Concrete(Los Alamos (MCNP) Mix rho=2.25 g/cc
8016.80c -0.511670
14028.80c -0.360360
13027.80c -0.0355
11023.80c -0.015270
20040.80c -0.05791
26054.80c -0.013780

C ~~~ CRITICALITY CODE ~~~~~
C

Kcode 10000 1 150 800 \$ KCODE (# of Neutrons/Cycle) (Initial keff guess) (# of
skipped cycles)(# of total cycles)

C # of Neutrons/Cycle Recommended 10³ for simple geometries; 10⁶ for complex

C Initial keff guess – Usually 1

C # of Skipped Cycles – 10% of Total Cycles

C # of Total Cycles – More cycles decreases error
ksrc -12 0 0 \$ KSRC x y z x y z ...
print, end of card

MICROREACTOR CORE, BURN 600
C
C ~~~~~ CELL CARD

~~~~~  
C Cylinder Pin 1, the Fully Ceramic Micro-Encapsulated Fuel  
1 1 -10.96 -1 u=1 tmp=5.1702E-08 imp:n=1 VOL=60821.2 \$UO2 without the  
TRISO components, universe 1 (T=600k)  
2 2 -2.577 1 -2 u=1 tmp=5.1702E-08 imp:n=1 \$TRISO shielding components,  
universe 1 (T=600k)  
3 6 -1.70 2 u=1 tmp=7.7553E-08 imp:n=1 \$outside of layer (T=900k)  
C Cylinder 2 air cooled system  
4 3 -0.001293 -3 u=2 tmp=5.1702E-08 imp:n=1 \$air flow, universe 2 (T=600k)  
5 4 -8 3 -4 u=2 tmp=5.1702E-08 imp:n=1 \$Steel pipe, universe 2 (T=600k)  
6 6 -1.70 4 u=2 tmp=7.7553E-08 imp:n=1 \$outside of layer (T=900k)  
C Center movement device  
7 5 -5.61 -5 u=3 tmp=5.1702E-08 imp:n=1 \$Zirconium Hydride, Universe 3  
(T=600k)  
8 4 -8 5 -6 u=3 tmp=5.1702E-08 imp:n=1 \$Steel pipe, universe 3 (T=600k)  
9 6 -1.70 6 u=3 tmp=7.7553E-08 imp:n=1 \$outside of layer(T=900k)

c -----  
10 7 -2.25 -7 8 -9 10 u=4 imp:n=1 lat=1 fill=-9:9 -9:9 0:0 \$square lattice-cell  
4 4 4 4 4 4 4 4 4 4 4 4 4 4 4 4 4 4  
4 4 4 4 4 4 4 4 4 4 4 4 4 4 4 4 4 4  
4 4 4 4 4 4 4 4 4 4 4 4 4 4 4 4 4 4  
4 4 4 1 1 1 1 1 1 1 1 1 1 1 1 1 1 4 4 4  
4 4 4 1 1 1 1 1 1 1 1 1 1 1 1 1 1 4 4 4  
4 4 4 1 1 2 1 1 1 1 1 1 1 1 2 1 1 4 4 4  
4 4 4 1 1 1 1 1 1 1 1 1 1 1 1 1 1 4 4 4  
4 4 4 1 1 1 1 2 1 1 1 2 1 1 1 1 1 4 4 4  
4 4 4 1 1 1 1 1 1 1 1 1 1 1 1 1 1 4 4 4  
4 4 4 1 1 1 1 1 1 1 1 1 1 1 1 1 1 4 4 4  
4 4 4 1 1 1 1 1 1 1 1 1 1 1 1 1 1 4 4 4  
4 4 4 1 1 1 1 1 1 1 1 1 1 1 1 1 1 4 4 4  
4 4 4 1 1 2 1 1 1 1 1 1 1 1 2 1 1 4 4 4  
4 4 4 1 1 1 1 1 1 1 1 1 1 1 1 1 1 4 4 4  
4 4 4 1 1 1 1 1 1 1 1 1 1 1 1 1 1 4 4 4  
4 4 4 4 4 4 4 4 4 4 4 4 4 4 4 4 4 4 4 4  
4 4 4 4 4 4 4 4 4 4 4 4 4 4 4 4 4 4 4 4  
4 4 4 4 4 4 4 4 4 4 4 4 4 4 4 4 4 4 4 4

11 6 -1.70 -11 12 -13 14 17 -18 tmp=7.7553E-08 imp:n=1 fill=4 \$square assembly

```

12 7 -2.25 -11 12 -13 14 -15 80 imp:n=1 $bottom concrete
13 7 -2.25 -11 12 -13 14 16 -90 imp:n=1 $top concrete
14 6 -1.70 -11 12 -13 14 15 -17 tmp=7.7553E-08 imp:n=1 $bottom moderator
15 6 -1.70 -11 12 -13 14 18 -16 tmp=7.7553E-08 imp:n=1 $top moderator
16 0 11:-12:13:-14:-80:90 imp:n=0 $Outside World

```

C Line above is blank delimiter.

C ~~~~~ SURFACE CARD

```

~~~~~
1 cz 0.55 $cm inner cylinder of UO2
2 cz 1.95 $cm outer layer of fcm pellet
3 cz 3 $cm inner cylinder of the moderator
4 cz 4 $cm layer of aluminum pipe
5 cz 3 $cm inner layer of the ZrH
6 cz 4 $cm outer layer of the ZrH
7 px 6.0 $1st side of the square lattice
8 px -6.0 $2nd side of the square lattice
9 py 6.0 $3rd side of the square lattice
10 py -6.0 $4th side of the square lattice
11 px 110.3 $1st side of the square assembly
12 px -110.3 $2nd side of the square assembly
13 py 110.3 $3rd side of the square assembly
14 py -110.3 $4th side of the square assembly
15 pz -210 $bottom of conc
16 pz 210 $top of conc
17 pz -200 $bottom of reflector
18 pz 200 $top of reflector
80 pz -230 $bottom of reflector
90 pz 230 $top of reflector

```

C Line above is blank delimiter.

C ~~~~~ MATERIAL CARD

```

~~~~~
C (Material#) (Fraction + Atomic - Weight) (include sources)
C Material entries must start in the column 6
BURN  TIME= 365 365 365 365 MAT = 1 Power =5
      BOPT=1.0 11 1 OMIT=1,8,6014,7016,8018,9018,13026,13028,14027,16031
MPHYS ON
m1  92235.81c 0.202 $Uranium 235 inside fuel kernel rho=10.96 g/cm^3,20%
      8016.81c 2.0 $Oxygen inside fuel kernel+PyC
      92238.81c 0.798 $Uranium 238 inside fuel kernel
mt1  o2-u.23t $material card
m2  6000.81c -0.45735 $Carbon Buffer layers 45.735 rho=0.98 g/cm^3
      1001.81c -0.06030 $Hydrogen from PyC 6.030
      14028.81c -0.44481 $Solid Silicon Carbide+Silicon Matrix rho=3.20g/cm^3
      8016.81c -0.03754 $Oxygen from PyC+SiC coatings

```



```
6 6 -1.70 4 u=2 tmp=7.7553E-08 imp:n=1 $outside of layer (T=900k)
C Center movement device
7 5 -5.61 -5 u=3 tmp=5.1702E-08 imp:n=1 $Zirconium Hydride, Universe 3
(T=600k)
8 4 -8 5 -6 u=3 tmp=5.1702E-08 imp:n=1 $Steel pipe, universe 3 (T=600k)
9 6 -1.70 6 u=3 tmp=7.7553E-08 imp:n=1 $outside of layer(T=900k)
c -----
10 7 -2.25 -7 8 -9 10 u=4 imp:n=1 lat=1 fill=-9:9 -9:9 0:0 $square lattice-cell
4 4 4 4 4 4 4 4 4 4 4 4 4 4 4 4 4 4 4 4 4 4 4 4 4 4 4 4 4 4 4 4 4 4 4 4 4 4
4 4 4 4 4 4 4 4 4 4 4 4 4 4 4 4 4 4 4 4 4 4 4 4 4 4 4 4 4 4 4 4 4 4 4 4 4 4
4 4 4 4 4 4 4 4 4 4 4 4 4 4 4 4 4 4 4 4 4 4 4 4 4 4 4 4 4 4 4 4 4 4 4 4 4 4
4 4 4 1 1 1 1 1 1 1 1 1 1 1 1 1 1 1 1 1 1 1 1 1 1 1 1 1 1 1 1 4 4 4 4
4 4 4 1 1 1 1 1 1 1 1 1 1 1 1 1 1 1 1 1 1 1 1 1 1 1 1 1 1 1 1 4 4 4 4
4 4 4 1 1 2 1 1 1 1 1 1 1 1 1 1 1 2 1 1 1 1 4 4 4 4
4 4 4 1 1 1 1 1 1 1 1 1 1 1 1 1 1 1 1 1 1 1 4 4 4 4
4 4 4 1 1 1 1 2 1 1 1 1 2 1 1 1 1 1 1 1 4 4 4 4
4 4 4 1 1 1 1 1 1 1 1 1 1 1 1 1 1 1 1 1 1 1 4 4 4 4
4 4 4 1 1 1 1 1 1 1 1 3 1 1 1 1 1 1 1 1 1 1 4 4 4 4
4 4 4 1 1 1 1 1 1 1 1 1 1 1 1 1 1 1 1 1 1 1 4 4 4 4
4 4 4 1 1 1 1 2 1 1 1 1 2 1 1 1 1 1 1 1 4 4 4 4
4 4 4 1 1 1 1 1 1 1 1 1 1 1 1 1 1 1 1 1 1 1 4 4 4 4
4 4 4 1 1 1 1 1 1 1 1 1 1 1 1 1 1 1 1 1 1 1 4 4 4 4
4 4 4 4 4 4 4 4 4 4 4 4 4 4 4 4 4 4 4 4 4 4 4 4 4 4 4 4 4 4 4 4 4 4 4 4 4 4
4 4 4 4 4 4 4 4 4 4 4 4 4 4 4 4 4 4 4 4 4 4 4 4 4 4 4 4 4 4 4 4 4 4 4 4 4 4
4 4 4 4 4 4 4 4 4 4 4 4 4 4 4 4 4 4 4 4 4 4 4 4 4 4 4 4 4 4 4 4 4 4 4 4 4 4
11 6 -1.70 -11 12 -13 14 17 -18 tmp=7.7553E-08 imp:n=1 fill=4 $square assembly
12 7 -2.25 -11 12 -13 14 -15 80 imp:n=1 $bottom concrete
13 7 -2.25 -11 12 -13 14 16 -90 imp:n=1 $top concrete
14 6 -1.70 -11 12 -13 14 15 -17 tmp=7.7553E-08 imp:n=1 $bottom moderator
15 6 -1.70 -11 12 -13 14 18 -16 tmp=7.7553E-08 imp:n=1 $top moderator
16 0 11:-12:13:-14:-80:90 imp:n=0 $Outside World
```

C Line above is blank delimiter.

C ~~~~~ SURFACE CARD

```
~~~~~
1 cz 0.55 $cm inner cylinder of UO2
2 cz 1.95 $cm outer layer of fcm pellet
3 cz 3 $cm inner cylinder of the moderator
4 cz 4 $cm layer of aluminum pipe
5 cz 3 $cm inner layer of the ZrH
6 cz 4 $cm outer layer of the ZrH
7 px 6.0 $1st side of the square lattice
8 px -6.0 $2nd side of the square lattice
9 py 6.0 $3rd side of the square lattice
```

10 py -6.0 \$4th side of the square lattice  
 11 px 110.3 \$1st side of the square assembly  
 12 px -110.3 \$2nd side of the square assembly  
 13 py 110.3 \$3rd side of the square assembly  
 14 py -110.3 \$4th side of the square assembly  
 15 pz -210 \$bottom of conc  
 16 pz 210 \$top of conc  
 17 pz -200 \$bottom of reflector  
 18 pz 200 \$top of reflector  
 80 pz -230 \$bottom of reflector  
 90 pz 230 \$top of reflector

C Line above is blank delimiter.

C ~~~~~ MATERIAL CARD

~~~~~

C (Material#) (Fraction + Atomic - Weight) (include sources)

C Material entries must start in the column 6

BURN TIME= 365 365 365 365 MAT = 1 Power =5

BOPT=1.0 11 1 OMIT=1,8,6014,7016,8018,9018,13026,13028,14027,16031

MPHYS ON

m1 92235.81c 0.202 \$Uranium 235 inside fuel kernel rho=10.96 g/cm<sup>3</sup>,20%

8016.81c 2.0 \$Oxygen inside fuel kernel+PyC

92238.81c 0.798 \$Uranium 238 inside fuel kernel

mt1 o2-u.23t \$material card

m2 6000.81c -0.45735 \$Carbon Buffer layers 45.735 rho=0.98 g/cm<sup>3</sup>

1001.81c -0.06030 \$Hydrogen from PyC 6.030

14028.81c -0.44481 \$Solid Silicon Carbide+Silicon Matrix rho=3.20g/cm<sup>3</sup>

8016.81c -0.03754 \$Oxygen from PyC+SiC coatings

m3 5010.82c -0.1442 5011.82c -0.6382 6000.82c -0.2176 \$boron carbide rho=-2.52

m4 14028.81c -0.01

24050.81c -0.19

28058.81c -0.095

26054.81c -0.705 \$Steel, Stainless 304L rho=8 g/cm<sup>3</sup>

m5 40090.81c -0.498

40091.81c -0.112

40092.81c -0.17

40094.81c -0.175

40096.81c -0.028

1001.81c -0.017 \$Zirconium Hydride rho=5.61 g/cm<sup>3</sup>

m6 6000.82c -1 \$Graphite core rho=1.70 g/cc

mt6 grph.26t \$Change for different temperatures

m7 1001.80c -0.004529 \$Concrete(Los Alamos (MCNP) Mix rho=2.25 g/cc

8016.80c -0.511670

14028.80c -0.360360

13027.80c -0.0355

11023.80c -0.015270

```

20040.80c -0.05791
26054.80c -0.013780
C ~ ~ ~ CRITICALITY CODE ~ ~ ~ ~ ~ ~ ~ ~ ~ ~ ~ ~ ~ ~ ~ ~ ~ ~ ~ ~ ~ ~ ~
C
kcode 10000 1 150 800 $ KCODE (# of Neutrons/Cycle) (Initial keff guess) (# of skipped
cycles)(# of total cycles)
C # of Neutrons/Cycle Recommended 10^3 for simple geometries; 10^6 for complex
C Initial keff guess – Usually 1
C # of Skipped Cycles – 10% of Total Cycles
C # of Total Cycles – More cycles decreases error
ksrc -12 0 0 $ KSRC x y z x y z ...
print, end card

```

## Appendix D: Output Results Matrix

Appendix D includes manipulation matrices and graphs containing the most reactive burn cases at 2.5, 5, and 7 MW with decay time up to 4 years. Graphs with and without control rods inserted are included. The full list of output matrices used for input can be found in the OUTPUT.ZIP file.

**Table D.1: Size Comparison**

| Size Comparison            |         |
|----------------------------|---------|
| Scale compared to original | Kcalc   |
| 0.75                       | 0.96274 |
| 1.5                        | 0.97285 |
| 2                          | 0.90623 |

**Table D.2: Control Rod Comparison**

| Control Rod Half Insertion Comparison |         |
|---------------------------------------|---------|
| NO CR:                                | 1.0159  |
| Half CR:                              | 0.99725 |

**Table D.3: Comparison of Fuel Levels**

| Comparison of Fuel Levels       |         |
|---------------------------------|---------|
| Less Fuel Diameter(0.35cm)      | 0.74091 |
| Baseline Fuel Diameter (0.55cm) | 1.0159  |
| More Fuel Diameter (0.95cm)     | 1.31135 |

**Table D.4: Control Rod Enrichment Comparison**

| Comparison of Enriched B4C |               |
|----------------------------|---------------|
|                            | $k_{eff}$     |
| Without Enrichment         | 0.93064       |
| With Enrichment            | 0.94259       |
| Difference                 | $\pm 0.01195$ |



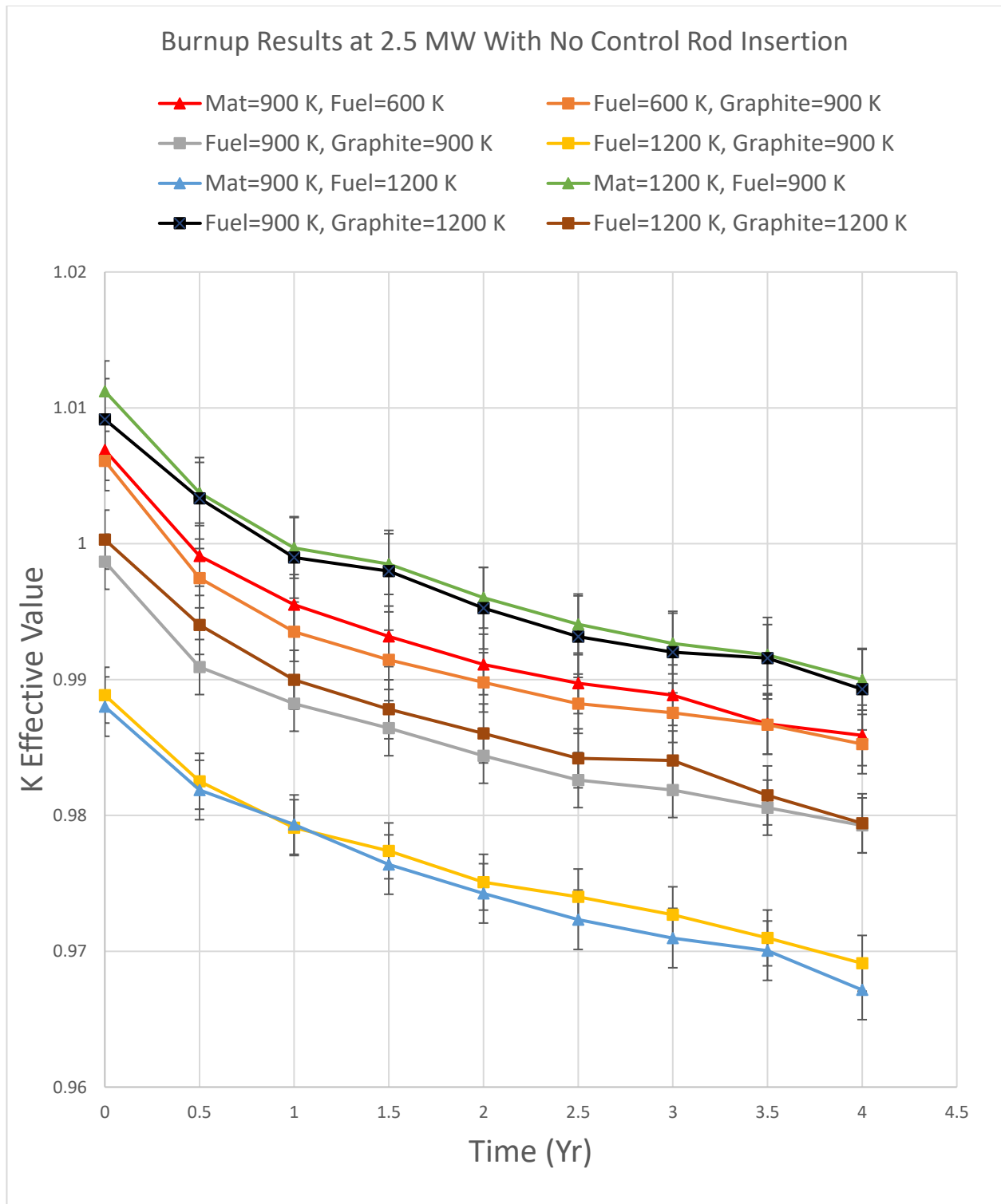


**Figure D.1: Burnup Results at 2.5 MW With No Control Rod Insertion**

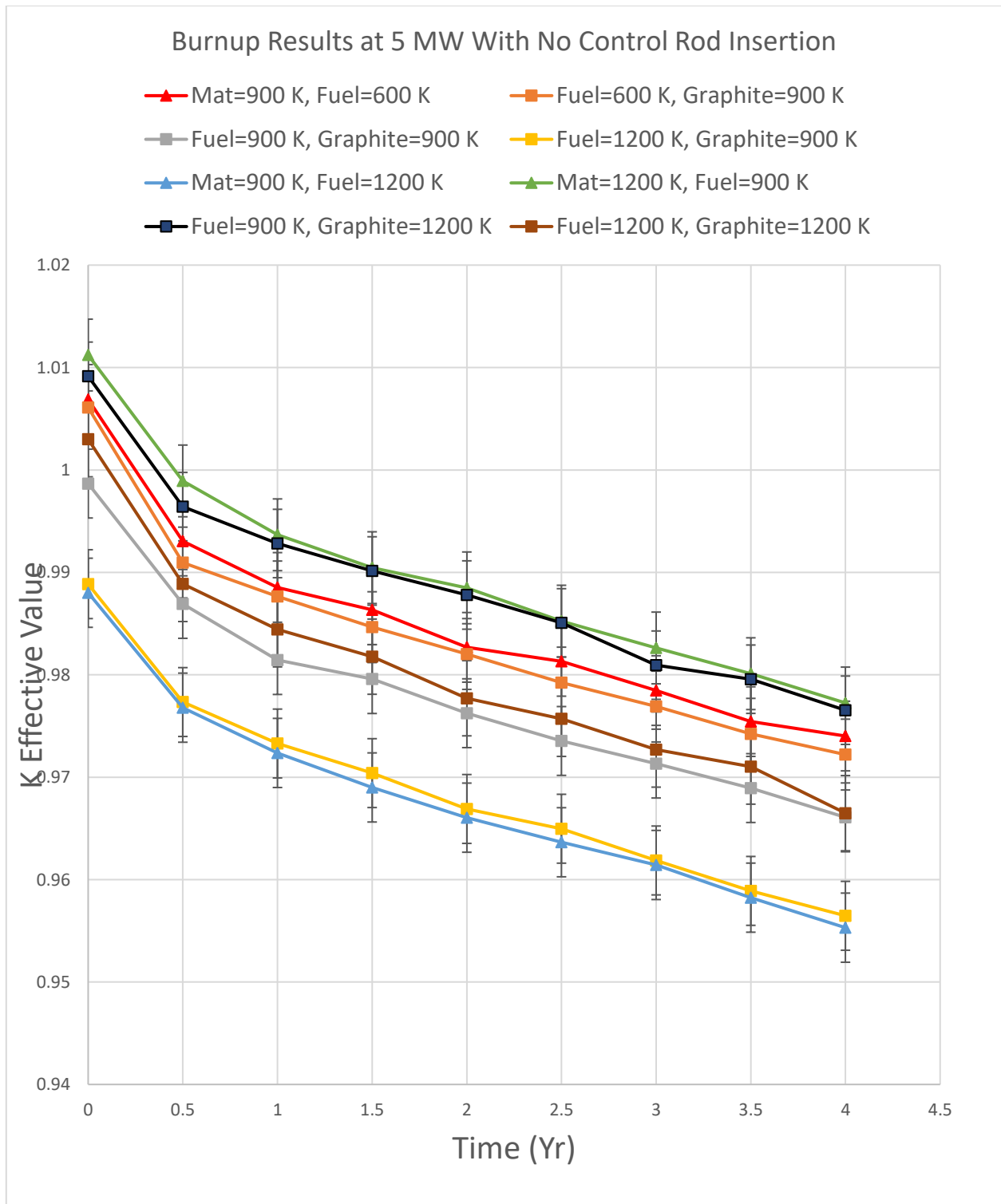


**Figure D.2: Burnup Results at 5 MW With No Control Rod Insertion**

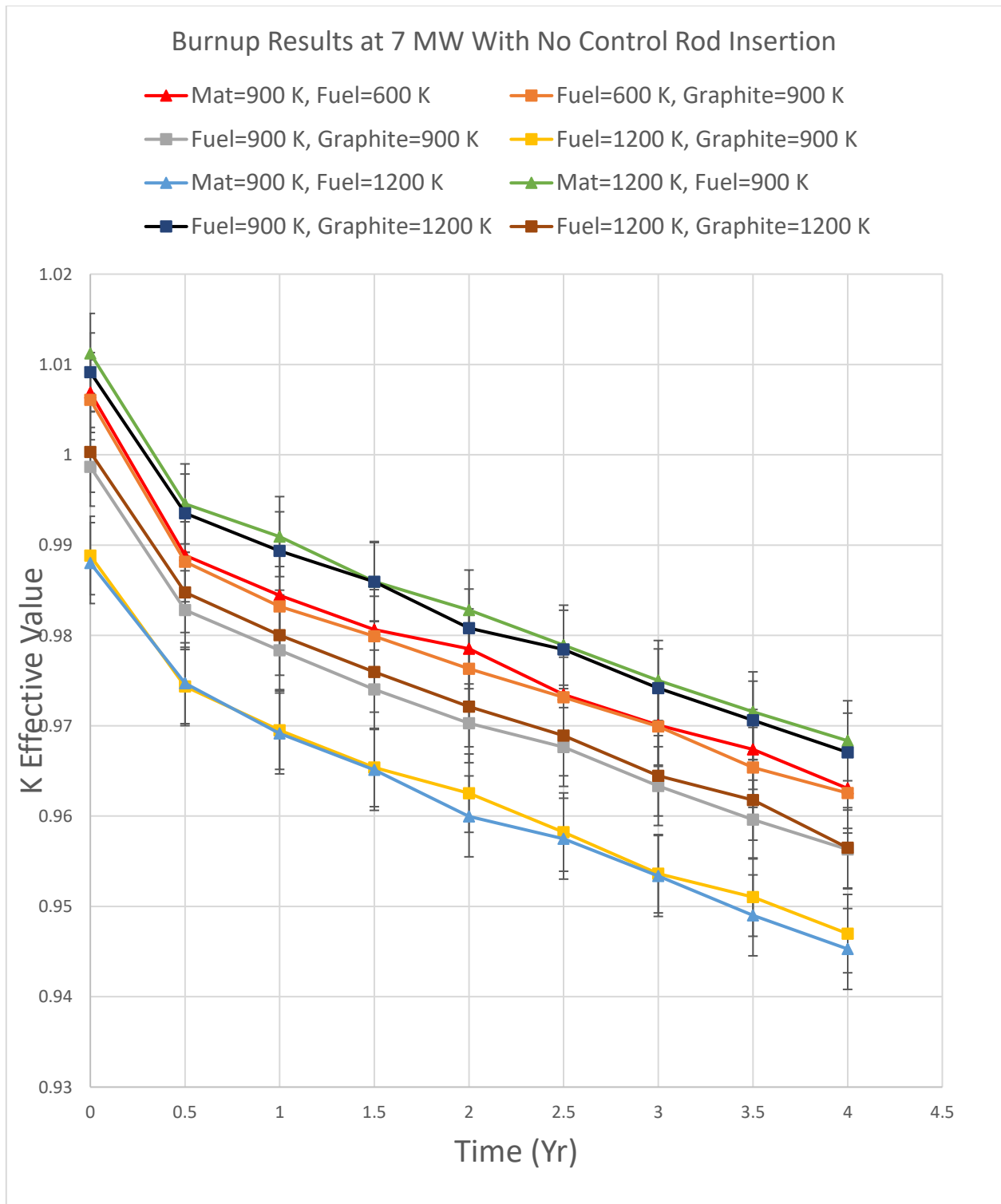


**Figure D.3: Burnup Results at 7 MW With No Control Rod Insertion**

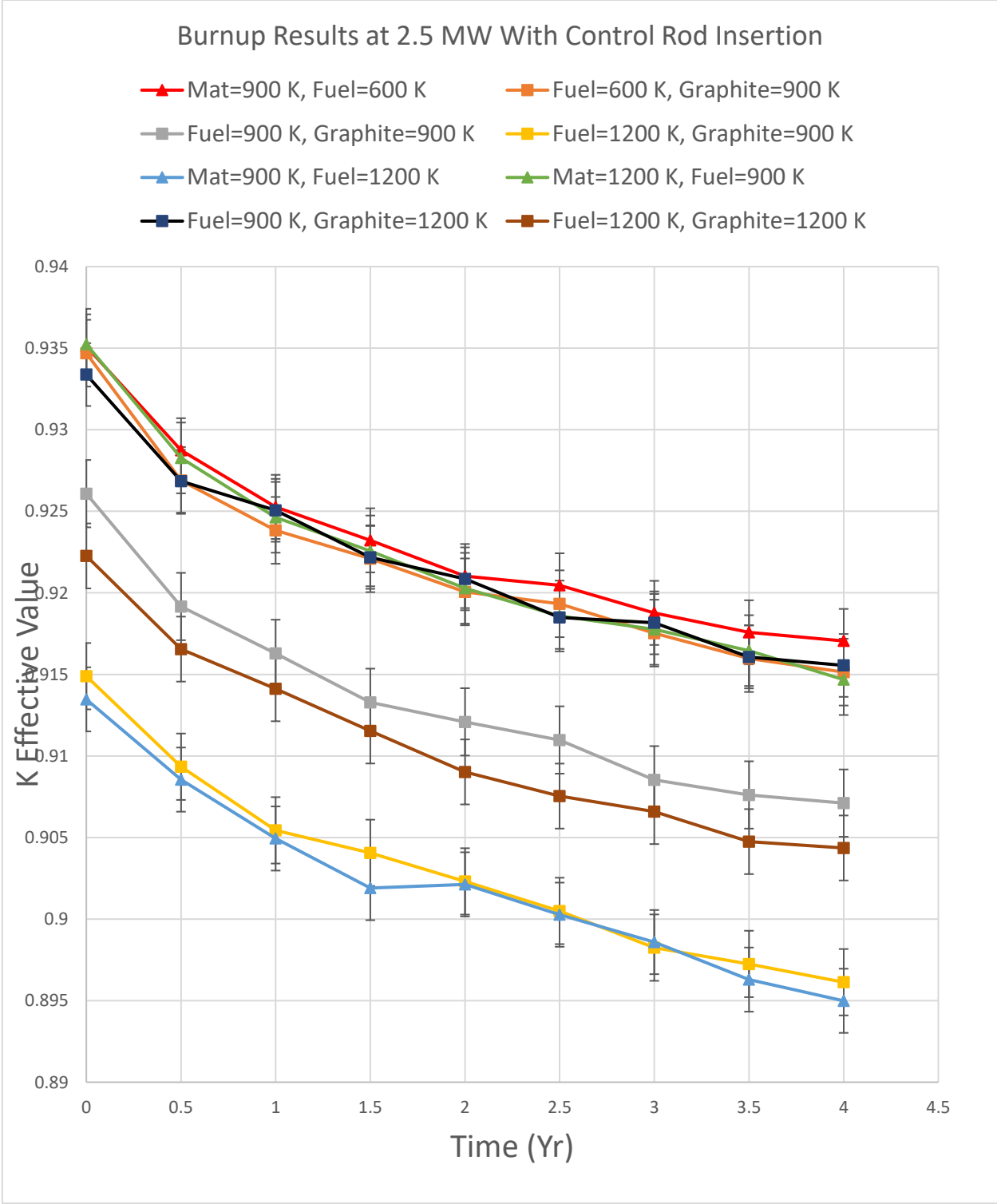


**Figure D.4 Burnup Results at 2.5 MW With Control Rod Insertion**

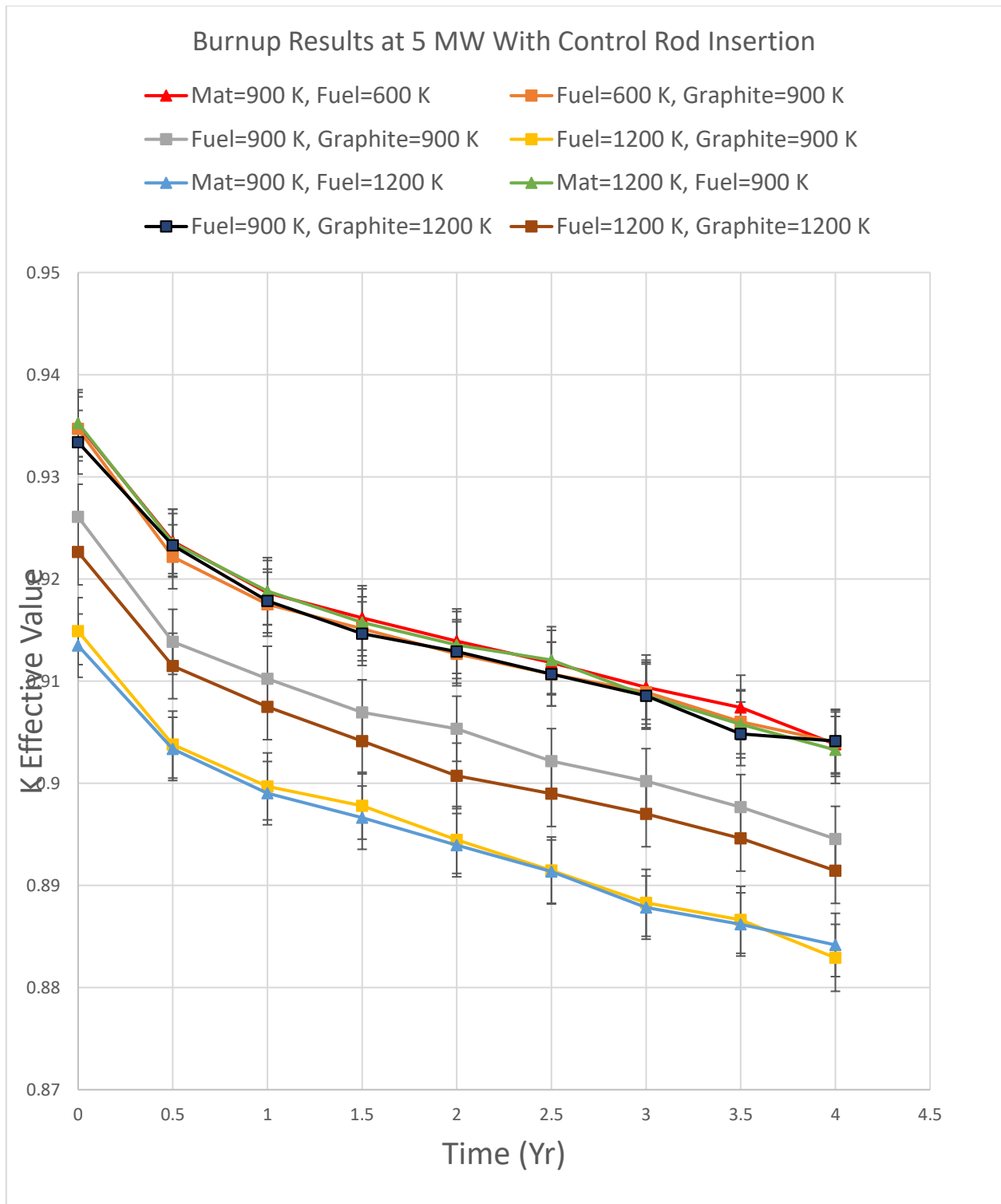


**Figure D.5: Burnup Results at 5 MW With Control Rod Insertion**

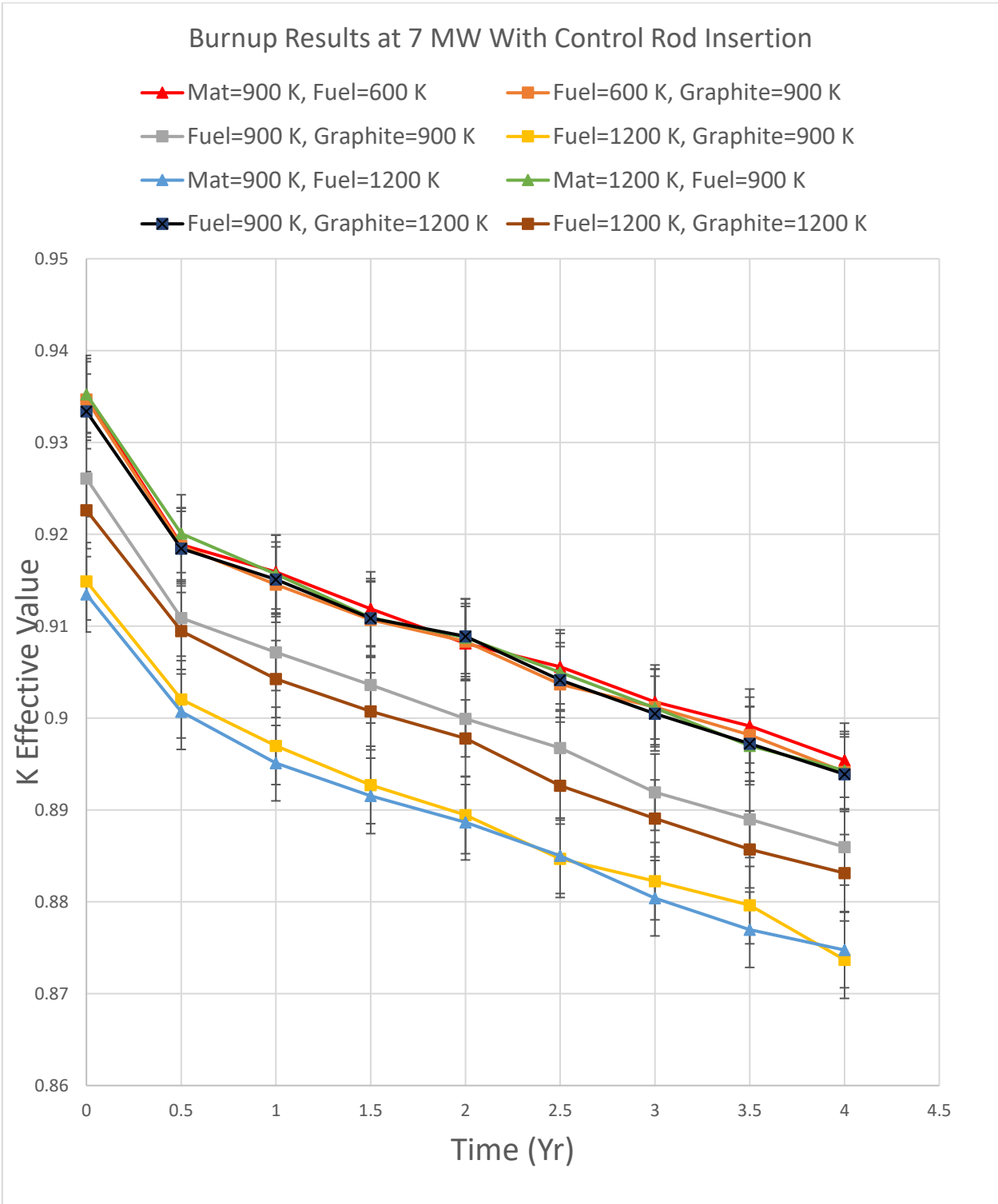


**Figure D.6: Burnup Results at 7 MW With Control Rod Insertion**

## Appendix E: Tally Case Results

Room Temperature Tallies (case 1) are included to compare against fuel (case 2) and graphite (case 3) T=1200k conditions.

Case 1:

1tally 4 nps = 4125206  
tally type 4 track length estimate of particle flux.  
particle(s): neutrons  
number of histories used for normalizing tallies = 3000000.00

volumes

cell: 1  
4.77280E+04

cell 1

multiplier bin: 4.77280E+04  
energy  
0.0000E+00 0.00000E+00 0.0000  
2.2222E+00 1.11608E+00 0.0006  
4.4444E+00 1.96447E-01 0.0015  
6.6667E+00 4.43217E-02 0.0032  
8.8889E+00 9.00143E-03 0.0073  
1.1111E+01 1.64263E-03 0.0171  
1.3333E+01 2.86571E-04 0.0375  
1.5556E+01 5.64649E-05 0.0864  
1.7778E+01 9.02587E-06 0.1888  
2.0000E+01 2.27366E-06 0.3645  
total 1.36785E+00 0.0005

cell 1

multiplier bin: -4.77280E+04 1 -6  
energy  
0.0000E+00 0.00000E+00 0.0000  
2.2222E+00 3.77631E-01 0.0008  
4.4444E+00 3.26078E-03 0.0015  
6.6667E+00 7.47086E-04 0.0032  
8.8889E+00 2.42955E-04 0.0073  
1.1111E+01 4.66072E-05 0.0171  
1.3333E+01 8.03070E-06 0.0376  
1.5556E+01 1.85120E-06 0.0874  
1.7778E+01 3.25713E-07 0.1889  
2.0000E+01 8.26582E-08 0.3635

total 3.81938E-01 0.0008

cell 1

multiplier bin: -4.77280E+04 1 -6 -7

energy

0.0000E+00 0.00000E+00 0.0000

2.2222E+00 9.20816E-01 0.0008

4.4444E+00 8.99735E-03 0.0015

6.6667E+00 2.33874E-03 0.0033

8.8889E+00 8.43440E-04 0.0073

1.1111E+01 1.76797E-04 0.0171

1.3333E+01 3.31175E-05 0.0377

1.5556E+01 8.26047E-06 0.0879

1.7778E+01 1.55445E-06 0.1894

2.0000E+01 4.18484E-07 0.3624

total 9.33216E-01 0.0008

cell 1

multiplier bin: -4.77280E+04 1 -2

energy

0.0000E+00 0.00000E+00 0.0000

2.2222E+00 8.95958E-02 0.0009

4.4444E+00 1.84014E-04 0.0022

6.6667E+00 1.27368E-04 0.0043

8.8889E+00 4.40518E-05 0.0077

1.1111E+01 1.68740E-05 0.0172

1.3333E+01 3.67578E-06 0.0377

1.5556E+01 5.71607E-07 0.0856

1.7778E+01 6.33438E-08 0.1843

2.0000E+01 1.23785E-08 0.3601

total 8.99724E-02 0.0009

volumes

cell: 3

2.43360E+06

cell 3

multiplier bin: 2.43360E+06

energy

0.0000E+00 0.00000E+00 0.0000

2.2222E+00 1.73706E+02 0.0004

4.4444E+00 3.06993E+00 0.0015



6.6667E+00 7.14513E-01 0.0035  
8.8889E+00 1.34777E-01 0.0079  
1.1111E+01 2.17883E-02 0.0178  
1.3333E+01 4.10394E-03 0.0419  
1.5556E+01 7.63128E-04 0.0985  
1.7778E+01 1.09085E-04 0.2540  
2.0000E+01 4.28506E-05 0.3707  
total 1.77652E+02 0.0004

cell 3

multiplier bin: -2.43360E+06 6 -1

energy

0.0000E+00 0.00000E+00 0.0000  
2.2222E+00 6.82021E+01 0.0004  
4.4444E+00 4.88755E-01 0.0015  
6.6667E+00 7.70224E-02 0.0035  
8.8889E+00 1.29494E-02 0.0079  
1.1111E+01 2.27162E-03 0.0178  
1.3333E+01 4.81776E-04 0.0419  
1.5556E+01 8.89586E-05 0.0982  
1.7778E+01 1.34408E-05 0.2553  
2.0000E+01 5.38440E-06 0.3706  
total 6.87837E+01 0.0004

cell 3

multiplier bin: -2.43360E+06 6 -3

energy

0.0000E+00 0.00000E+00 0.0000  
2.2222E+00 6.81752E+01 0.0004  
4.4444E+00 4.88750E-01 0.0015  
6.6667E+00 7.14089E-02 0.0035  
8.8889E+00 9.84086E-03 0.0079  
1.1111E+01 1.28143E-03 0.0178  
1.3333E+01 3.06607E-04 0.0420  
1.5556E+01 5.73143E-05 0.0980  
1.7778E+01 8.90101E-06 0.2564  
2.0000E+01 3.45963E-06 0.3702  
total 6.87468E+01 0.0004

cell 3

multiplier bin: -2.43360E+06 6 -2

energy

|            |             |        |
|------------|-------------|--------|
| 0.0000E+00 | 0.00000E+00 | 0.0000 |
| 2.2222E+00 | 2.68938E-02 | 0.0007 |
| 4.4444E+00 | 5.78930E-06 | 0.0015 |
| 6.6667E+00 | 6.40568E-06 | 0.0086 |
| 8.8889E+00 | 3.71549E-04 | 0.0113 |
| 1.1111E+01 | 3.30160E-04 | 0.0183 |
| 1.3333E+01 | 3.24792E-05 | 0.0424 |
| 1.5556E+01 | 4.36219E-06 | 0.0990 |
| 1.7778E+01 | 7.31893E-07 | 0.2539 |
| 2.0000E+01 | 3.91358E-07 | 0.3708 |
| total      | 2.76457E-02 | 0.0007 |

Case 2:

volumes

cell: 1  
4.77280E+04

cell 1

multiplier bin: 4.77280E+04

energy

|            |             |        |
|------------|-------------|--------|
| 0.0000E+00 | 0.00000E+00 | 0.0000 |
| 2.2222E+00 | 1.11357E+00 | 0.0006 |
| 4.4444E+00 | 1.96855E-01 | 0.0015 |
| 6.6667E+00 | 4.43788E-02 | 0.0032 |
| 8.8889E+00 | 8.93820E-03 | 0.0072 |
| 1.1111E+01 | 1.71106E-03 | 0.0164 |
| 1.3333E+01 | 3.31079E-04 | 0.0387 |
| 1.5556E+01 | 5.55457E-05 | 0.0933 |
| 1.7778E+01 | 1.08576E-05 | 0.2015 |
| 2.0000E+01 | 8.86560E-07 | 0.5371 |
| total      | 1.36585E+00 | 0.0005 |

cell 1

multiplier bin: -4.77280E+04 1 -6

energy

|            |             |        |
|------------|-------------|--------|
| 0.0000E+00 | 0.00000E+00 | 0.0000 |
| 2.2222E+00 | 3.76814E-01 | 0.0008 |
| 4.4444E+00 | 3.26741E-03 | 0.0015 |
| 6.6667E+00 | 7.48276E-04 | 0.0033 |
| 8.8889E+00 | 2.41070E-04 | 0.0072 |

|            |             |        |
|------------|-------------|--------|
| 1.1111E+01 | 4.85537E-05 | 0.0164 |
| 1.3333E+01 | 9.27454E-06 | 0.0387 |
| 1.5556E+01 | 1.80448E-06 | 0.0929 |
| 1.7778E+01 | 3.91549E-07 | 0.2014 |
| 2.0000E+01 | 3.25030E-08 | 0.5375 |
| total      | 3.81130E-01 | 0.0008 |

cell 1

multiplier bin: -4.77280E+04      1      -6      -7

energy

|            |             |        |
|------------|-------------|--------|
| 0.0000E+00 | 0.00000E+00 | 0.0000 |
| 2.2222E+00 | 9.18825E-01 | 0.0008 |
| 4.4444E+00 | 9.01660E-03 | 0.0015 |
| 6.6667E+00 | 2.34245E-03 | 0.0033 |
| 8.8889E+00 | 8.36495E-04 | 0.0072 |
| 1.1111E+01 | 1.84076E-04 | 0.0164 |
| 1.3333E+01 | 3.82237E-05 | 0.0387 |
| 1.5556E+01 | 8.02004E-06 | 0.0928 |
| 1.7778E+01 | 1.86465E-06 | 0.2007 |
| 2.0000E+01 | 1.66200E-07 | 0.5381 |
| total      | 9.31253E-01 | 0.0008 |

cell 1

multiplier bin: -4.77280E+04      1      -2

energy

|            |             |        |
|------------|-------------|--------|
| 0.0000E+00 | 0.00000E+00 | 0.0000 |
| 2.2222E+00 | 9.13516E-02 | 0.0009 |
| 4.4444E+00 | 1.84378E-04 | 0.0022 |
| 6.6667E+00 | 1.27947E-04 | 0.0044 |
| 8.8889E+00 | 4.37128E-05 | 0.0076 |
| 1.1111E+01 | 1.76033E-05 | 0.0169 |
| 1.3333E+01 | 4.27476E-06 | 0.0402 |
| 1.5556E+01 | 5.62565E-07 | 0.0941 |
| 1.7778E+01 | 7.90945E-08 | 0.2131 |
| 2.0000E+01 | 5.21397E-09 | 0.5428 |
| total      | 9.17302E-02 | 0.0009 |

volumes

cell:      3  
            2.43360E+06

cell 3

multiplier bin: 2.43360E+06  
 energy  
 0.0000E+00 0.00000E+00 0.0000  
 2.2222E+00 1.73524E+02 0.0004  
 4.4444E+00 3.06863E+00 0.0015  
 6.6667E+00 7.12685E-01 0.0035  
 8.8889E+00 1.35008E-01 0.0079  
 1.1111E+01 2.21829E-02 0.0178  
 1.3333E+01 4.09637E-03 0.0409  
 1.5556E+01 7.80674E-04 0.0941  
 1.7778E+01 1.08781E-04 0.2230  
 2.0000E+01 1.22290E-05 0.4919  
 total 1.77468E+02 0.0004

cell 3  
 multiplier bin: -2.43360E+06 6 -1  
 energy  
 0.0000E+00 0.00000E+00 0.0000  
 2.2222E+00 6.66961E+01 0.0004  
 4.4444E+00 4.88385E-01 0.0015  
 6.6667E+00 7.68496E-02 0.0035  
 8.8889E+00 1.28958E-02 0.0079  
 1.1111E+01 2.30758E-03 0.0178  
 1.3333E+01 4.81287E-04 0.0409  
 1.5556E+01 9.14998E-05 0.0942  
 1.7778E+01 1.33915E-05 0.2224  
 2.0000E+01 1.54158E-06 0.4928  
 total 6.72771E+01 0.0004

cell 3  
 multiplier bin: -2.43360E+06 6 -3  
 energy  
 0.0000E+00 0.00000E+00 0.0000  
 2.2222E+00 6.66693E+01 0.0004  
 4.4444E+00 4.88379E-01 0.0015  
 6.6667E+00 7.12530E-02 0.0035  
 8.8889E+00 9.80054E-03 0.0079  
 1.1111E+01 1.30128E-03 0.0179  
 1.3333E+01 3.06478E-04 0.0410  
 1.5556E+01 5.91250E-05 0.0943  
 1.7778E+01 8.86437E-06 0.2225

2.0000E+01 9.96405E-07 0.4931  
total 6.72404E+01 0.0004

cell 3

multiplier bin: -2.43360E+06 6 -2  
energy  
0.0000E+00 0.00000E+00 0.0000  
2.2222E+00 2.68498E-02 0.0007  
4.4444E+00 5.78685E-06 0.0015  
6.6667E+00 6.42327E-06 0.0086  
8.8889E+00 3.65281E-04 0.0114  
1.1111E+01 3.35531E-04 0.0182  
1.3333E+01 3.22256E-05 0.0413  
1.5556E+01 4.44869E-06 0.0944  
1.7778E+01 7.25004E-07 0.2284  
2.0000E+01 1.11505E-07 0.4937  
total 2.76004E-02 0.0007

Case 3: volumes

cell: 1  
4.77280E+04

cell 1

multiplier bin: 4.77280E+04  
energy  
0.0000E+00 0.00000E+00 0.0000  
2.2222E+00 1.14506E+00 0.0006  
4.4444E+00 1.97120E-01 0.0015  
6.6667E+00 4.44704E-02 0.0032  
8.8889E+00 9.01144E-03 0.0072  
1.1111E+01 1.72468E-03 0.0167  
1.3333E+01 3.10639E-04 0.0365  
1.5556E+01 5.37808E-05 0.0882  
1.7778E+01 5.85598E-06 0.2148  
2.0000E+01 1.70655E-06 0.3781  
total 1.39775E+00 0.0005

cell 1

multiplier bin: -4.77280E+04 1 -6  
energy  
0.0000E+00 0.00000E+00 0.0000

|            |             |        |
|------------|-------------|--------|
| 2.2222E+00 | 4.07963E-01 | 0.0007 |
| 4.4444E+00 | 3.27191E-03 | 0.0015 |
| 6.6667E+00 | 7.49667E-04 | 0.0033 |
| 8.8889E+00 | 2.43248E-04 | 0.0072 |
| 1.1111E+01 | 4.89374E-05 | 0.0167 |
| 1.3333E+01 | 8.70909E-06 | 0.0365 |
| 1.5556E+01 | 1.76249E-06 | 0.0886 |
| 1.7778E+01 | 2.11296E-07 | 0.2149 |
| 2.0000E+01 | 6.21572E-08 | 0.3800 |
| total      | 4.12288E-01 | 0.0007 |

cell 1

|                 |              |        |    |    |
|-----------------|--------------|--------|----|----|
| multiplier bin: | -4.77280E+04 | 1      | -6 | -7 |
| energy          |              |        |    |    |
| 0.0000E+00      | 0.00000E+00  | 0.0000 |    |    |
| 2.2222E+00      | 9.94728E-01  | 0.0007 |    |    |
| 4.4444E+00      | 9.02777E-03  | 0.0015 |    |    |
| 6.6667E+00      | 2.34650E-03  | 0.0033 |    |    |
| 8.8889E+00      | 8.44327E-04  | 0.0072 |    |    |
| 1.1111E+01      | 1.85592E-04  | 0.0167 |    |    |
| 1.3333E+01      | 3.58770E-05  | 0.0365 |    |    |
| 1.5556E+01      | 7.86224E-06  | 0.0889 |    |    |
| 1.7778E+01      | 1.01329E-06  | 0.2150 |    |    |
| 2.0000E+01      | 3.14595E-07  | 0.3824 |    |    |
| total           | 1.00718E+00  | 0.0007 |    |    |

cell 1

|                 |              |        |    |
|-----------------|--------------|--------|----|
| multiplier bin: | -4.77280E+04 | 1      | -2 |
| energy          |              |        |    |
| 0.0000E+00      | 0.00000E+00  | 0.0000 |    |
| 2.2222E+00      | 9.58953E-02  | 0.0009 |    |
| 4.4444E+00      | 1.84068E-04  | 0.0022 |    |
| 6.6667E+00      | 1.28042E-04  | 0.0043 |    |
| 8.8889E+00      | 4.40037E-05  | 0.0077 |    |
| 1.1111E+01      | 1.76731E-05  | 0.0169 |    |
| 1.3333E+01      | 3.97890E-06  | 0.0367 |    |
| 1.5556E+01      | 5.44968E-07  | 0.0885 |    |
| 1.7778E+01      | 3.88710E-08  | 0.2177 |    |
| 2.0000E+01      | 9.63352E-09  | 0.3877 |    |
| total           | 9.62737E-02  | 0.0008 |    |

volumes

cell: 3  
2.43360E+06

cell 3  
multiplier bin: 2.43360E+06  
energy  
0.0000E+00 0.00000E+00 0.0000  
2.2222E+00 1.71984E+02 0.0004  
4.4444E+00 3.06855E+00 0.0015  
6.6667E+00 7.15817E-01 0.0035  
8.8889E+00 1.34819E-01 0.0080  
1.1111E+01 2.21505E-02 0.0177  
1.3333E+01 3.98947E-03 0.0405  
1.5556E+01 7.39471E-04 0.0960  
1.7778E+01 1.02170E-04 0.2693  
2.0000E+01 3.87178E-05 0.3614  
total 1.75930E+02 0.0004

cell 3  
multiplier bin: -2.43360E+06 6 -1  
energy  
0.0000E+00 0.00000E+00 0.0000  
2.2222E+00 6.60640E+01 0.0004  
4.4444E+00 4.88509E-01 0.0015  
6.6667E+00 7.71918E-02 0.0035  
8.8889E+00 1.28901E-02 0.0079  
1.1111E+01 2.30836E-03 0.0177  
1.3333E+01 4.68572E-04 0.0404  
1.5556E+01 8.62802E-05 0.0961  
1.7778E+01 1.24866E-05 0.2686  
2.0000E+01 4.83751E-06 0.3629  
total 6.66454E+01 0.0004

cell 3  
multiplier bin: -2.43360E+06 6 -3  
energy  
0.0000E+00 0.00000E+00 0.0000  
2.2222E+00 6.60472E+01 0.0004  
4.4444E+00 4.88503E-01 0.0015  
6.6667E+00 7.15878E-02 0.0035  
8.8889E+00 9.80497E-03 0.0079

|            |             |        |
|------------|-------------|--------|
| 1.1111E+01 | 1.30255E-03 | 0.0177 |
| 1.3333E+01 | 2.98428E-04 | 0.0404 |
| 1.5556E+01 | 5.55934E-05 | 0.0963 |
| 1.7778E+01 | 8.21532E-06 | 0.2685 |
| 2.0000E+01 | 3.10610E-06 | 0.3643 |
| total      | 6.66188E+01 | 0.0004 |

cell 3

multiplier bin: -2.43360E+06      6      -2

energy

|            |             |        |
|------------|-------------|--------|
| 0.0000E+00 | 0.00000E+00 | 0.0000 |
| 2.2222E+00 | 1.67119E-02 | 0.0006 |
| 4.4444E+00 | 5.78670E-06 | 0.0015 |
| 6.6667E+00 | 6.48374E-06 | 0.0086 |
| 8.8889E+00 | 3.62772E-04 | 0.0113 |
| 1.1111E+01 | 3.34208E-04 | 0.0181 |
| 1.3333E+01 | 3.12965E-05 | 0.0407 |
| 1.5556E+01 | 4.21581E-06 | 0.0951 |
| 1.7778E+01 | 7.07126E-07 | 0.2769 |
| 2.0000E+01 | 3.55030E-07 | 0.3605 |
| total      | 1.74578E-02 | 0.0007 |



## Bibliography

- [1] Department of Energy. (2021, March 31). *How much power does a nuclear reactor produce?*. Energy.gov. <https://www.energy.gov/ne/articles/infographic-how-much-power-does-nuclear-reactor-produce>
- [2] Lamarsh, J. R., & Baratta, A. J. (2001). 7.4. In *Introduction to Nuclear Engineering* (Third, pp. 365–374). essay, Prentice Hall.
- [3] Gralla, F., Abson, D. J., Møller, A. P., Lang, D. J., & von Wehrden, H. (2017b). Energy transitions and National Development Indicators: A global review of nuclear energy production. *Renewable and Sustainable Energy Reviews*, 70, 1251–1265. <https://doi.org/10.1016/j.rser.2016.12.026>
- [4] California Independent System Operator. (2023). *Understanding electricity*. California ISO - Understanding electricity. <https://www.caiso.com/about/Pages/OurBusiness/Understanding-electricity.aspx>
- [5] MacDonald, S., Winner, B., Smith, L., Juillerat, J., & Belknap, S. (2019, June 14). *Bridging the rural efficiency gap: Expanding access to energy efficiency upgrades in remote and high energy cost communities - energy efficiency*. SpringerLink. <https://link.springer.com/article/10.1007/s12053-019-09798-8>
- [6] U.S. Government Accountability Office. (2009, February). *Defense Management: DOD needs to increase attention on fuel demand management at forward-deployed locations*. Defense Management: DOD Needs to Increase Attention on Fuel Demand Management at Forward-Deployed Locations | U.S. GAO. <https://www.gao.gov/products/gao-09-300>
- [7] Brown, F., Rising, M., & Alwin, J. (2017). *User Manual for Whisper-1.1*. Los Alamos National Laboratory. [https://mcnp.lanl.gov/pdf\\_files/la-ur-17-20567.pdf](https://mcnp.lanl.gov/pdf_files/la-ur-17-20567.pdf)
- [8] Beneš, O., Gilbert, A. Q., Hernández, F. A., Oladokun, V. O., Peakman, A., & Straub, J. (2021, June 12). *Review of nuclear microreactors: Status, potentialities and challenges*. *Progress in Nuclear Energy*. <https://www.sciencedirect.com/science/article/abs/pii/S0149197021001888?via%3Dihub>
- [9] INL Media. (2023, November 8). *EBR-I lights up the history of nuclear energy development*. Idaho National Laboratory. <https://inl.gov/history-of-inl/ebr-i-lights-up-the-history-of-nuclear-energy-development/>
- [10] Amy, J. (2023, February 17). *Georgia nuclear plant again delayed at cost of \$200m more*. AP News. <https://apnews.com/article/georgia-power-co-southern-climate-and-environment-business-3b1d6c65353c6a65b1ccfdede753ab7>
- [11] Alguacil, J., Sauvan, P., Juarez, R., & Catalan, J. P. (2018). Assessment and optimization of MCNP memory management for detailed geometry of nuclear fusion facilities. *Fusion Engineering and Design*, 136, 386–389. <https://doi.org/10.1016/j.fusengdes.2018.02.048>

- [12] McDowell, B. K., Nickolaus, J. R., Mitchell, M. R., Swearingen, G. L., & Pugh, R. (2015). High Temperature Gas Reactors: Assessment of Applicable Codes and Standards. <https://doi.org/10.2172/1031438>
- [13] US Government of Accountability Office. (2022). *GAO-22-105394, nuclear energy projects: DOE should institutionalize ...* GAO Assets. <https://www.gao.gov/assets/gao-22-105394.pdf>
- [14] Waksman, J. (2022, May). *Project Pele Overview - NRC*. Project Pele Overview. <https://www.nrc.gov/docs/ML2212/ML22126A059.pdf>
- [15] Los Alamos National Laboratory. (2011). ENDF71X: Nuclear data. ENDF71x | Nuclear Data. <https://nucleardata.lanl.gov/ace/endf71x/>
- [16] World Nuclear Association. (2021, August). Fast Neutron Reactors. Fast Neutron Reactors | FBR - World Nuclear Association. <https://world-nuclear.org/information-library/current-and-future-generation/fast-neutron-reactors.aspx>
- [17] Jud, S. (2022, June 9). BWXT Technologies. BWXT to Build First Advanced Microreactor in United States. <https://www.bwxt.com/news/2022/06/09/BWXT-to-Build-First-Advanced-Microreactor-in-United-States>
- [18] Detwiler, R. S., McConn, R. J., Grimes, T. F., Upton, S. A., & Engel, E. J. (2021, April 1). Compendium of material composition data for Radiation Transport Modeling. Compendium of Material Composition Data for Radiation Transport Modeling (Technical Report) | OSTI.GOV. <https://www.osti.gov/biblio/1782721>
- [19] Trejo, F. C., Padilla, M. S., & López-Honorato, E. (2015). Understanding the 1600°C fuel temperature limit of TRISO coated fuel particles. MRS Proceedings, 1769. <https://doi.org/10.1557/opl.2015.119>
- [20] Sanders, C. E., & Wagner, J. C. (2001). Parametric study of the effect of burnable poison rods for PWR Burnup Credit. NUREG/CR-6759 . <https://doi.org/10.2172/814219>
- [21] Starcore. (2022, December 1). Starcore Nuclear Technology. StarCore Nuclear. <https://starcorenuclearpower.com/technology/>
- [22] X Energy. (2024). Xe-Mobile - Advanced Micro-Mobile Nuclear Reactor Solutions - X-energy. Reactor: Xe-Mobile. <https://x-energy.com/reactors/xe-mobile>
- [23] McLaughlin, T. P., Monahan, S., Pruvost, N. L., Frolov, V. V., Ryazanov, B. G., & Sviridov, V. I. (2000). A review of criticality accidents 2000 revision. A Review of Criticality Accidents, (2000 Revision). <https://doi.org/10.2172/758324>

- [24] Wallenius, j. (2017). Sealer: A small lead-cooled reactor for power production in the ... - IAEA. IAEA-International Nuclear Information System.  
[https://inis.iaea.org/collection/NCLCollectionStore/\\_Public/49/086/49086085.pdf?r=1](https://inis.iaea.org/collection/NCLCollectionStore/_Public/49/086/49086085.pdf?r=1)
- [25] World Nuclear Association. (2023, October). Small Nuclear Power Reactors. Small nuclear power reactors - World Nuclear Association. <https://www.world-nuclear.org/information-library/nuclear-fuel-cycle/nuclear-power-reactors/small-nuclear-power-reactors.aspx> Known Critical Experiments for Code
- [26] James L. Everett III, The first prototype high temperature gas cooled reactor (HTGR) was successfully developed. (2003, August 12). *Peach Bottom Unit No. 1: A high performance helium cooled nuclear power plant*. Annals of Nuclear Energy.  
<https://www.sciencedirect.com/science/article/abs/pii/S0306454978900178>
- [27] Schwarz. (2018). The visual editor for MCNPX.  
<http://www.mcnpvised.com/visualeditor/visualeditor.html>
- [28] Marciulescu, C. (2019). EPRI-ar-1(NP)-A, “Uranium Oxycarbide (UCO) tristructural isotropic (triso)-coated particle fuel performance”, part 3 of 3. Electric Power Research Institute.  
<https://www.nrc.gov/docs/ML2033/ML20336A056.html>
- [29] Cardis, E., & Hatch, M. (2011). The Chernobyl Accident — An Epidemiological Perspective. *Clinical Oncology (Royal College of Radiologists (Great Britain))*, 23(4), 251–260.  
<https://doi.org/10.1016/j.clon.2011.01.510>
- [30] Bot, P. L., Boutin, P., Lorigny, J., & Hutchins, E. (2003, October 21). *Human reliability data, human error and accident models-illustration through the Three Mile Island accident analysis*. Reliability Engineering & System Safety.  
<https://www.sciencedirect.com/science/article/abs/pii/S0951832003002035?via%3Dihub>
- [31] Haghghat, A. (2021). Monte Carlo Methods for Particle Transport. CRC Press. Graph Figure Citation
- [32] USNRC HRTD. (2011, September). General Electric Systems Technology manual Chapter 1.7 Reactor Physics. Nuclear Regulatory Commission.  
<https://www.nrc.gov/docs/ML1125/ML11258A296.pdf>
- [33] “International Handbook of Evaluated Criticality Safety Benchmark Experiments” Nuclear Energy Agency (May 2020)
- [34] U.S. Nuclear Regulatory Commission. (2001, January). NUREG/CR-6698 Guide for Validation of Nuclear Criticality Safety Calculational Methodology.  
<https://www.nrc.gov/docs/ML0502/ML050250061.pdf>

- [35] Baumer, R., Xu, Y., Minato, K., Petti, D. A., Liu, B., Maki, J. T., Miller, G. K., Sawa, K., Ogawa, T., Bullock, R. E., Morimoto, K., Snead, L. L., Martin, D. G., Kupitz, J., & Chen, F. (2010, July 30). *A review of Triso Fuel Performance models*. Journal of Nuclear Materials. <https://www.sciencedirect.com/science/article/abs/pii/S0022311510003284?via%3Dihub>  
<https://www.usnc.com/fuel/>
- [36] Brown, Nicholas R., Hernandez, Richard, & Nelson, Andrew T. (2022, April) High volume packing fraction TRISO-based fuel in light water reactors. United States. <https://doi.org/10.1016/j.pnucene.2022.104151>
- [37] Westinghouse Nuclear. (2024, January). Energy Systems. <https://www.westinghousenuclear.com/energy-systems/evinci-microreactor>
- [38] Brown, F., & Martin, W. (2005, April). La-UR-04-8668 - STOCHASTIC GEOMETRY AND HTGR MODELING WITH MCNP5. STOCHASTIC GEOMETRY AND HTGR MODELING WITH MCNP5. [https://mcnp.lanl.gov/pdf\\_files/TechReport\\_2004\\_LANL\\_LA-UR-04-8668\\_BrownMartinEtAl.pdf](https://mcnp.lanl.gov/pdf_files/TechReport_2004_LANL_LA-UR-04-8668_BrownMartinEtAl.pdf)
- [39] Arafat, Y., & Van Wyk, J. (2019). Our Next Disruptive Technology. Nuclear Plant Journal, (March-April 2019), 34–37.
- [40] C.J. Werner (editor), (2017), "MCNP Users Manual - Code Version 6.2, Appendix G", LA-UR-17-29981
- [41] Ultra Safe Nuclear. (2023, October 10). Triso and FCM Fuel. <https://www.usnc.com/fuel/>
- [42] C.J. Werner (editor), (2017), "MCNP Users Manual - Code Version 6.2", LA-UR-17-29981
- [43] <https://www.osti.gov/servlets/purl/1323135> (use for another database option)
- [44] [multimedia.3m.com/mws/media/950554O/3m-10b-enriched-boron-carbide-data-sheet.pdf?&fn=EnrichedBoronCarbide10B\\_Celum\\_9803052\\_R4.pdf](https://multimedia.3m.com/mws/media/950554O/3m-10b-enriched-boron-carbide-data-sheet.pdf?&fn=EnrichedBoronCarbide10B_Celum_9803052_R4.pdf) (USE FOR BORON CARBIDE)
- [45] Robb, S., & Koroush, S. (2023). Construction schedule and cost risk for large and small light water reactors. Nuclear Engineering and Design, 407. <https://doi.org/10.1016/j.nucengdes.2023.112305>
- [46] Testoni, R., Bersano, A., & Segantin, S. (2021). Review of nuclear microreactors: Status, potentialities and challenges. Progress in Nuclear Energy, 138. <https://doi.org/10.1016/j.pnucene.2021.103822>

- [47] SUGAWARA, S. (2023). Towards “extended” safety goals (conceptual exploration of safety goals for microreactors). *Mechanical Engineering Journal-The Japan Society of Mechanical Engineers*. <https://doi.org/10.1299/mej.23-00375>
- [48] Colombo, M., & Fairweather, M. (2021). Study of nuclear reactor external vessel passive cooling using computational fluid dynamics. *Nuclear Engineering and Design*, 378. <https://doi.org/10.1016/j.nucengdes.2021.111186>
- [49] Fensin, M., Hendricks, J., & McKinney, G. (2009, April). Monte Carlo Burnup Interactive tutorial - mcnp.lanl.gov. American Nuclear Society . [https://mcnp.lanl.gov/pdf\\_files/TechReport\\_2009\\_LANL\\_LA-UR-09-02051\\_FensinHendricksEtAl.pdf](https://mcnp.lanl.gov/pdf_files/TechReport_2009_LANL_LA-UR-09-02051_FensinHendricksEtAl.pdf)
- [50] Maldonado, A., & Perfetti, C. (2023). Utilizing sensitivity and correlation coefficients from MCNP and whisper to guide Microreactor experiment design. *Nuclear Science and Engineering*, 197(8), 2086–2098. <https://doi.org/10.1080/00295639.2022.2162782>
- [51] Koreshi, Z. (2022). *Nuclear engineering mathematical modeling and simulation*. Academic Press.
- [52] Greenwood, N. (1997). *Chemistry of the elements* (2nd edition). Butterworth-Heinemann.
- [53] Knief, R. A. (2003). Nuclear power reactors. *Encyclopedia of Physical Science and Technology*, 739–761. <https://doi.org/10.1016/b0-12-227410-5/00495-6>
- [54] Foulon, F., Badeau, G., Dubois, M., & Safieh, J. (1970, January 1). Study of temperature effects on Ulysse reactor for training and qualification of Operating Personnel. [inis.iaea.org. https://inis.iaea.org/search/search.aspx?orig\\_q=RN%3A39043208](https://inis.iaea.org/search/search.aspx?orig_q=RN%3A39043208)
- [55] Touran, N. (2023). What is a nuclear moderator?. What is nuclear? <https://whatisnuclear.com/moderation.html>

## Curriculum Vitae

**Cameron Jensen**  
Camj1210@gmail.com

### SPECIALIZED SKILLS/STRENGTHS

---

**Software:** MATLAB, MCNP-6, SolidWorks, Autodesk Suite, Microsoft Office (PowerPoint, Excel, Word)

**Certifications:** EIT/FE (Nevada), OSHA 10-hour, SP-2 Certification

### EDUCATION

---

**University of Nevada Las Vegas, Las Vegas, NV, Master of Science in Nuclear Engineering, GPA: 3.68      June 2024** *Organizations:* Tau Beta Pi, Engineers Without Borders

**University of Nevada Las Vegas, Las Vegas, NV, Bachelor of Science in Mechanical Engineering, GPA: 3.45      May 2022**

*Honors and Awards:* Future Net Zero Innovators Symposium 2<sup>nd</sup> place, National Merit Corporation Scholarship Recipient, American Legion Award Recipient

### ENGINEERING EXPERIENCE

---

**Nuclear Engineer I – Probabilistic Risk Assessment, X Energy, Rockville, MD      June 2023-Current**

**Exp Engineering- Mechanical Engineering Intern November 2022-Current**

- Coordinates, designs, and manages multi-million-dollar commercial hospitality projects throughout the United States. Uses Autodesk Revit and Bluebeam to design mechanical and plumbing systems to exceed code standards.

**Love Engineering-Mechanical HVAC and Plumbing Designer      April 2019-Current**

- Executes MEP engineering and energy audits for residential, multi-family, and commercial buildings throughout the United States. Specializes in AutoCAD design and RHVAC/Ekotrope Report creation.

**Kittrell Jensen Contractors Field/Office Intern      June 2018-September 2018**

- Assisted on site superintendents with management of several projects at once; worked directly with project managers to create schedules for newly acquired bids; generated Sage Timberline files to execute project change orders, closeouts, and daily reports.